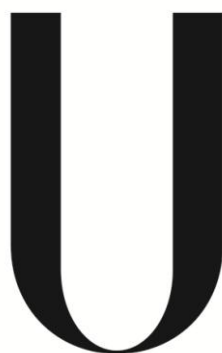


UNIVERSIDADE DE LISBOA  
FACULDADE DE CIÊNCIAS  
DEPARTAMENTO DE BIOLOGIA ANIMAL



LISBOA

---

UNIVERSIDADE  
DE LISBOA

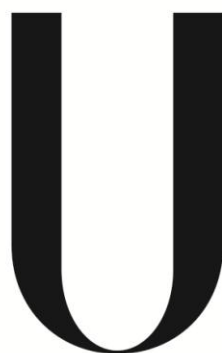
**Analysis of the molecular interactions between  
Msx1 and other key players during mouse limb  
development**

---

Joana Cristina Reino Carvalho

Dissertação  
Mestrado em Biologia Evolutiva e do Desenvolvimento  
2013

UNIVERSIDADE DE LISBOA  
FACULDADE DE CIÊNCIAS  
DEPARTAMENTO DE BIOLOGIA ANIMAL



LISBOA

---

UNIVERSIDADE  
DE LISBOA

**Analysis of the molecular interactions between  
Msx1 and other key players during mouse limb  
development**

---

Joana Cristina Reino Carvalho

**Dissertação orientada por:**  
**Doutor Benoît Robert**  
**Professora Doutora Sólveig Thorsteinsdóttir**

Dissertação  
Mestrado em Biologia Evolutiva e do Desenvolvimento  
2013



# Acknowledgements

First I would like to thank to all the people in the lab, especially Benoît my supervisor for his encouragement and suggestions and Mathura, whom I closely work with for helping me with pretty much everything inside and outside the bench throughout my internship.

To professor Sólveig, who accepted to be my internal supervisor and was always present and willing to offer her help whenever I had a doubt or problem.

Then I would like to thank to all my friends in Paris that made my life brighter and more enjoyable while I was in this new foreign country taken aback from my comfort zone and made me feel at home again. Thank you very much Fernando, Mathura, Jeremy and all the others that, one way or another, made me smile!

And finally a special thanks to all my family for their unconditional support throughout this whole journey. Without you, I wouldn't have made it this far. I love you all very much!

This is for all of you!

# Abstract

In vertebrates, the anteroposterior (AP) growth and patterning of the limb bud rely on an intricate regulatory genetic network involving Shh and Gli3. Although the mechanism allowing Shh to modulate Gli3 activity is well documented, the role of Msx genes, which constitute a small family of genes encoding homeodomain transcription factors that have been implicated in AP limb patterning, within this genetic network remains poorly understood. Based on empirical evidence generated by previous studies, we hypothesized that Msx genes may interact with the transcription factor Gli3, particularly, with its repressor form, Gli3R in order to drive limb morphogenesis. To test this hypothesis, we performed a series of protein interaction assays using the Proximity Ligation Assay (PLA) technique followed by quantification analysis. Using this technique we were able to produce evidence supporting our initial assumption admitting the *in vivo* interaction between the transcription factors Msx1 and Gli3R in the forelimb and hindlimb bud at 11.5 *dpc*. In parallel, we also investigated the involvement of these transcription factors in the BMP signaling pathway, by testing their ability to interact with the PSmad1,5,8 protein complex, the intracellular transducer of the BMP signaling cascade. Using the same experimental approach, we were able to demonstrate that both Msx1 and Gli3R interact with this protein complex in mesenchymal cells of the forelimb at 11.5 *dpc*. Based on these results and on the fact that the BMP signaling pathway has been systematically implicated in the apoptotic events taking place in the limb, together with the observation that the absence of Msx genes and/or Gli3 result in phenotypes concomitant with apoptosis impairment, we propose that Msx1, Gli3R and the Psmad1,5,8 proteins interact with each other in order to form a trimeric nuclear transcriptional complex that will drive the expression of BMP target genes involved in cell death regulation.

**Keywords:** Anteroposterior patterning | *Msx* genes | Gli3 | Limb development | BMP

## Resumo

Nos vertebrados, o crescimento e padronização anterior-posterior (AP) do botão do membro é regulado através de uma rede genética altamente complexa, cujos principais intervenientes incluem o fator parácrino *Sonic hedgehog* (Shh) e o fator de transcrição Gli3. A nível molecular, o principal papel do fator parácrino Shh durante o desenvolvimento do membro é contrabalançar a atividade do fator de transcrição Gli3, impedindo a formação de Gli3R, a forma truncada da proteína Gli3 que atua como um potente repressor transcrricional que se acumula principalmente nas células da região anterior do botão do membro que não expressam Shh (Wang *et al.*, 2000). Estas interações genéticas resultam na pré-padronização do botão do membro, definindo claramente duas regiões distintas: a região anterior, onde as células expressam altos níveis de Gli3R e baixos de Gli3A, e a região posterior que, uma vez que se encontra na proximidade da Zona de Atividade Polarizante (ZPA), o local de síntese do fator Shh, possui contrariamente à região anterior elevados níveis de Gli3A e baixos de Gli3R (Wang *et al.*, 2000; Zeller *et al.*, 2009).

Apesar do mecanismo envolvido na regulação da atividade do fator Gli3 através da sinalização Shh estar bem documentado na literatura, o papel dos genes *Msx*, que constituem uma pequena família de fatores de transcrição envolvidos na morfogénese e padronização AP do botão do membro, no âmbito desta rede genética ainda não é bem conhecido. Diversos estudos têm sugerido que os genes *Msx* desempenham um papel fundamental na morfogénese do membro, interagindo com o fator de transcrição Gli3, mais especificamente com a sua forma repressora Gli3R. A prova mais direta que aponta para a existência de uma interação entre estes dois genes foi obtida no laboratório a partir de uma experiência de co-imunoprecipitação (Co-IP) realizada num sistema *in vitro* constituído por células HEK293 que foram co-transfectadas com cDNAs codificantes dos alelos *Msx1* e Gli3R marcados com sequências *C-myc* e *Flag*, respetivamente. Os resultados obtidos posteriormente por Western Blot revelaram que era possível precipitar ambas as proteínas GLI3R e MSX1 utilizando anticorpos direcionados contra as sequências *C-myc* e *Flag* dos alelos *Msx1* e Gli3R respetivamente, indicando que estas proteínas têm capacidade de interagir uma com a outra nas condições experimentais estabelecidas neste sistema artificial (O. Goupille and B. Robert, unpublished data). Contudo, é importante salientar que neste sistema

artificial o nível de expressão destas proteínas não é controlado e pode, portanto, não corresponder aos níveis endógenos a que as células do botão do membro estão sujeitas *in vivo*. Assim, de modo a contornar este problema, é necessário estabelecer um sistema adequado que permita o estudo *in vivo* destas interações genéticas que ocorrem durante o desenvolvimento do membro embrionário, que constitui, no fundo, o principal objetivo do trabalho aqui apresentado.

Com a finalidade de investigar a relação entre os fatores de transcrição Msx1 e Gli3R *in vivo* utilizando o botão do membro como modelo experimental, começámos por gerar uma série de estirpes animais transgênicas, contendo construções genéticas que nos permitiriam detetar a existência de interações entre estes fatores de transcrição *in vivo*. Após o cruzamento destas linhagens transgênicas, gerámos embriões com 11 dias pós-coito heterozigóticos para *Prx1<sup>Cre/0</sup>*; *Msx1<sup>HA-His/+</sup>*; *Rosa<sup>Gli3R-Flag/+</sup>*; *Gli3<sup>Flox/+</sup>* nos quais realizámos uma série de experiências de interações entre proteínas, incluindo Co-IP e a técnica de Proximity Ligation Assay (PLA) seguida de uma análise estatística quantitativa. Através desta última foi possível demonstrar que os fatores de transcrição Msx1 e Gli3R interagem *in vivo* tanto nas células mesenquimais do membro anterior como do membro posterior aos 11 dias pós-coito.

Por outro lado, outros estudos focados no papel dos genes Msx e de componentes da cascata de sinalização BMP na formação do palato têm vindo a sugerir que estes genes interagem com elementos desta via de sinalização, que não o recetor *Bmpr1A*, de modo a promover a formação do palato (Liu *et al.*, 2005; Zhang *et al.*, 2002). Paralelamente, em 1998 Liu *et al.* demonstraram que num sistema *in vitro* constituído por células COS1 transfectadas com isoformas *full-length* ou truncadas da proteína Gli3, apenas as proteínas truncadas na sua extremidade carboxílica (estruturalmente semelhantes ao repressor transcricional Gli3R) tinham capacidade de se associar a proteínas Smad endógenas através do seu domínio *zinc-finger*, levantando assim a possibilidade de que as proteínas Gli poderão também interagir *in vivo* com esta mesma cascata de sinalização através das proteínas Smad. Com base nestes resultados, decidimos também investigar em mais detalhe o envolvimento destes fatores de transcrição na via de sinalização BMP, testando a sua capacidade de interagir com o complexo proteico PSmad1,5,8, o transdutor de sinal intracelular responsável pela regulação da transcrição de genes-alvo desta via de sinalização. Tirando partido da mesma abordagem experimental, conseguimos demonstrar que ambos os fatores de transcrição Msx1 e

Gli3R interagem com este complexo proteico nas células mesenquimais do membro anterior aos 11 dias pós-coito.

Após termos verificado que os fatores de transcrição Msx1 e Gli3R interagem um com o outro e que ambos estão envolvidos na cascata de sinalização BMP interagindo com o complexo proteico PSmad1,5,8, estávamos interessados em investigar os processos biológicos que têm lugar no botão do membro que poderiam ser controlados por estes complexos proteicos. Uma vez que já tinha sido demonstrado que mutantes *Gli3*<sup>-/-</sup> e *Msx1*<sup>-/-</sup>; *Msx2*<sup>+/-</sup> apresentam malformações nos membros provocadas pela não ocorrência de apoptose (Aoto *et al.*, 2002; Lallemand *et al.*, 2009), colocámos imediatamente a hipótese de que o fator de transcrição Msx1, juntamente com Gli3R e com o complexo proteico PSmad1,5,8 poderiam estar envolvidos no controlo da apoptose que tem lugar no botão do membro durante o desenvolvimento embrionário. De forma a investigar esta possibilidade e a confirmar que de facto os genes Msx estão envolvidos neste processo, realizámos uma série de experiências de imunofluorescência contra Caspase3 utilizando embriões *Msx1*<sup>-/-</sup>; *Msx2*<sup>-/-</sup> com o objetivo de avaliar o padrão de distribuição e intensidade da apoptose presente no botão do membro. Os resultados obtidos indicaram claramente que na ausência de Msx1 e Msx2, há uma diminuição drástica na morte celular programada na região anterior do botão do membro, confirmando assim que de facto estes genes são indispensáveis para a ocorrência de apoptose e, em última instância, para a morfogénese e padronização do botão do membro.

Tendo como base estes resultados, juntamente com o facto da via de sinalização BMP ter sido sistematicamente apontada como estando implicada na regulação da apoptose que tem lugar nas células mesenquimais do botão do membro de mamíferos e aves (Guha *et al.*, 2002; Yokouchi *et al.*, 1996; Zou and Niswander, 1996), acrescido ao facto de se ter demonstrado que a ausência de genes *Msx* e/ou *Gli3* resulta no aparecimento de anomalias provocadas pela diminuição e/ou ausência de morte celular programada no botão do membro (Aoto *et al.*, 2002; Lallemand *et al.*, 2009), propomos um modelo em que os fatores de transcrição Msx1 e Gli3R interagem com o complexo proteico PSmad1,5,8 de modo a formar um trímero nuclear transcrricional responsável pela indução de genes-alvo da cascata de sinalização BMP diretamente envolvidos no controlo da apoptose. Apesar de ter sido possível demonstrar através da PLA que existem interações entre estas três proteínas no botão do membro *in vivo*, muitos aspetos



relacionados com a sua natureza celular e molecular ficaram ainda por esclarecer. Assim, no futuro é necessário investigar estas interações proteicas em mais detalhe por forma a esclarecer, em primeiro lugar, qual é o papel desempenhado pelo fator de transcrição *Msx1* na apoptose mediada através da cascata de sinalização BMP. Em segundo lugar, descobrir quais os domínios e motivos proteicos que permitem a estas proteínas interagirem fisicamente umas com as outras. Em terceiro lugar, tentar perceber de que forma é que estas interações proteicas regulam a expressão de genes-alvo da via de sinalização BMP e quais são as consequências que isso acarreta em termos da morfogénese e padronização do membro. E, finalmente, investigar em mais detalhe de que modo é que a apoptose mediada através da cascata de sinalização BMP é regulada temporal e espacialmente e quais serão os outros fatores de transcrição e/ou cofatores envolvidos nesse processo.

**Palavras-chave:** Padronização anterior-posterior | Genes *Msx* | *Gli3* | Desenvolvimento do membro | BMP

# Table of Contents

Acknowledgements.....	3
Abstract.....	4
Resumo .....	5
I. Introduction .....	10
I.1. Vertebrate limb development .....	10
I.2. Anteroposterior growth and patterning of the limb bud .....	12
I.3. The Shh/Gli3/Msx regulatory genetic network .....	14
I.4. The involvement of Msx1 and Gli3R in the BMP signaling pathway .....	17
II. Objectives .....	19
III. Materials and Methods .....	20
III.1. Mouse strains and genotyping .....	20
III.2. LacZ staining .....	22
III.3. Alcian Blue cartilage staining .....	22
III.4. Alizarin Red skeletal staining .....	22
III.5. Limb bud protein extraction.....	23
III.6. Co-Immunoprecipitation (Co-IP) and Western Blotting .....	23
III.7. Proximity Ligation Assay (PLA) .....	23
III.8. Immunofluorescence.....	25
III.9. Statistical analysis.....	27
IV. Results .....	28
IV.1. Overexpression of Gli3R driven by <i>Prx1-Cre</i> causes limb defects.....	28
IV.2. Gli3R and MSX1 interact <i>in vivo</i> at E11.5 in the limb bud.....	29
IV.3. Gli3R and Msx1 interact with the BMP pathway through Smads.....	31
IV.4. Apoptosis is deregulated in the limb bud of <i>Msx1<sup>-/-</sup></i> ; <i>Msx2<sup>-/-</sup></i> .....	33
V. Discussion.....	35
V.1. The relationship between Msx1, Gli3R and the BMP cascade.....	35
V.2. Concluding remarks .....	39
References .....	40
Appendix I – Supplementary data .....	44
Appendix II – Solutions and buffers .....	45
Appendix III – Antibodies.....	48

# I. Introduction

The study of the complex processes and signaling networks underlying the development of an adult organism from the initial relative simplicity of a zygote could be defined as the main goal of Developmental Biology.

During development, the formation of a new organism results from the coordinated combination of multiple processes including growth, morphogenesis and cellular differentiation through a temporal and spatial regulation of gene expression and cell behaviour. However, the processes by which an undifferentiated field of cells acquire spatial pattern and undergo coordinated differentiation are not fully understood (Berge *et al.*, 2008; Ros and Fernandez-Teran, 2008).

The limb has long been a pioneering model system for examining the molecular mechanisms of tissue patterning and morphogenesis during development. The first genetic studies performed since the 1940s, focused mainly on elucidating the functions of a particular gene or pathway during limb bud development, but the challenge now is to understand how the genes and pathways interact to orchestrate limb organogenesis (Zeller *et al.*, 2009).

## I.1. Vertebrate limb development

In vertebrates, the developing limb emerges from the flank mesenchyme at predetermined positions along the embryonic axis. Around 9.5 *dpc* (*days post coitum*) in the mouse and 19HH in the chick, the forelimb buds arise from the embryo trunk at the level of the heart. In the mouse, about half a day later, the hindlimb buds begin to protrude near the posterior end of the embryo at the level of the kidneys (Taher *et al.*, 2011; Zeller *et al.*, 2009). At this stage each limb bud is composed of a meshwork of apparently homogeneous undifferentiated and highly proliferative mesenchymal cells derived from the lateral plate mesoderm (LPM) covered by the surface ectoderm, that colonize the limb field around E9.5 (HH19) up to E10.5 (HH22) (Taher *et al.*, 2011). The mesoderm contains the progenitors of skeletal elements, tendons and other connective tissues that will be present in the fully-formed limb, whereas the surface ectoderm gives rise to the skin and other cutaneous structures such as feathers on birds or hairs on mammals. Shortly after the limb buds emerge, changes in cell shape and

position within the surface ectoderm result in the appearance of a ridge around E10.5 (HH22), the apical ectodermal ridge (AER), which runs along the distal margin of each limb bud (Taher *et al.*, 2011; Towers and Tickle, 2009). This thickened specialized epithelium is required for limb bud outgrowth, as it produces signals that promote proximo-distal elongation. As the bud elongates, the cells near the body wall begin to differentiate, while the cells at the bud tip will remain undifferentiated. In the meantime, these mesenchymal cells start to form small compact aggregates called precartilaginous condensations that will prefigure the limb skeletal elements found in the adult. From E11.5 (HH25) up to E13.5 (HH32), the cartilage differentiates from the condensations, giving rise to the skeletal primordial. By E12.5 (HH29) the digits start to appear and from E13.5 onward, the cartilaginous skeleton starts to mineralize and is slowly replaced by bone tissue. Simultaneously, the limbs become vascularized, as they are invaded by blood vessels that will ensure a constant blood flow to maintain tissue viability during limb outgrowth (Hall and Miyake, 2000; Towers and Tickle, 2009) (Fig.1).

Immediately after the AER has formed, a second limb organizer emerges in the posterior region of the limb bud, the zone of polarizing activity (ZPA). It is the interplay between the AER, ZPA, ectoderm and the underlying mesenchyme that control the elongation along the proximo-distal (PD) axis

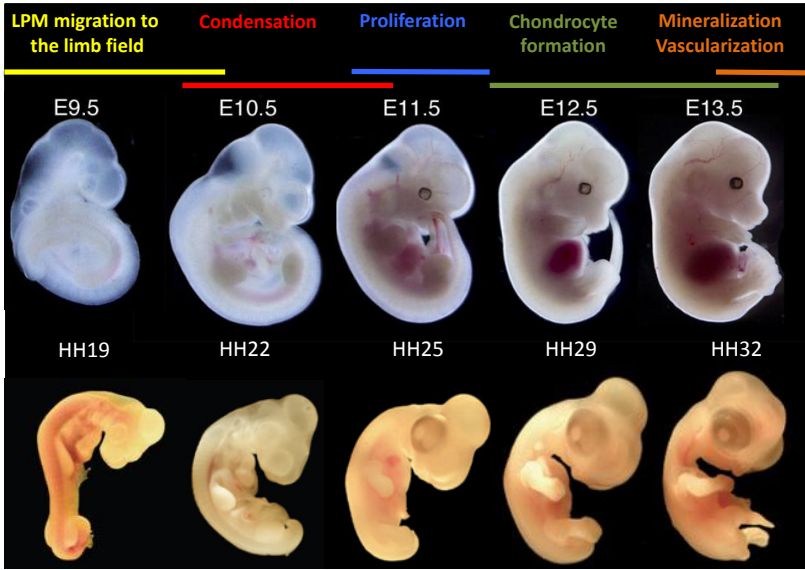


**Figure 1 Vertebrate limb development.** Overview of the main events taking place during vertebrate limb development as a function of developmental stage and model organism (mouse on the top panel and chick on the bottom panel). E, time in days following fertilization; HH, Hamburger and Hamilton developmental stages . Adapted from Taher *et al.*, 2011

(shoulder to fingers), the flattening along the dorso-ventral (DV) axis (back of hand to palm), the number, and the identity of digits along the antero-posterior (AP) axis (thumb to little finger) (Taher *et al.*, 2011) (Fig.2A). It takes seven days after the wing buds first

appear (and about five days in the mouse forelimb) for the complete skeleton to form, with the stylopod (humerus) forming first, followed by the intermediate segments composing the zeugopod (radius and ulna) and the distal autopod elements (wrist and digits) forming last (Towers and Tickle, 2009; Bénazet and Zeller, 2009) (Fig.2B).

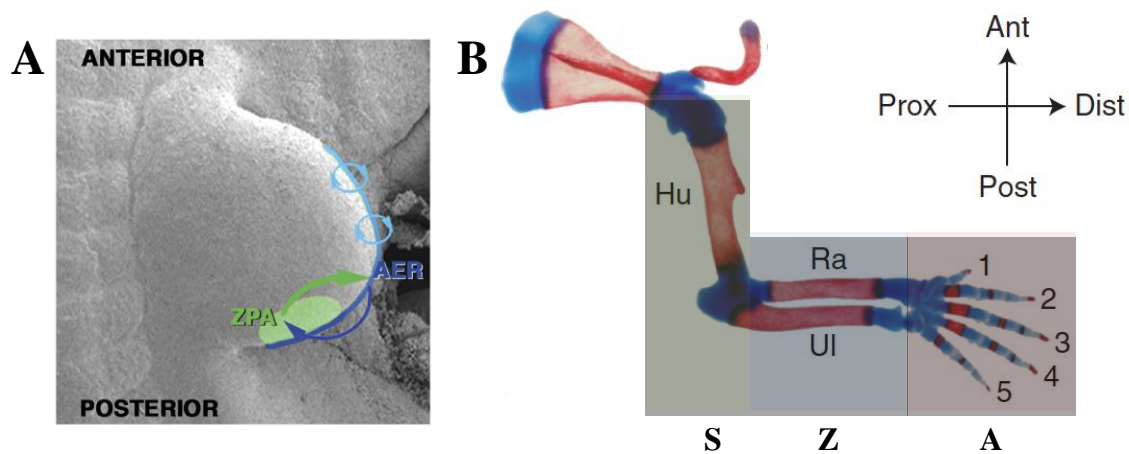


**Figure 2 Limb bud organization throughout development. (A) The limb bud organizers.** Scanning electron micrograph of a mouse limb bud showing the zone of polarizing activity (ZPA, in green) located in the posterior limb bud mesenchyme and the apical ectodermal ridge (AER, in blue). These two signaling centers communicate by reciprocal signaling interactions (arrows). **(B) Skeletal preparation of mouse forelimb stained with alcian blue and alizarin red at birth.** The stylopod (S, in green) gives rise to the most proximal limb skeletal element, the humerus (Hu). The zeugopod (Z, in blue) forms the radius (Ra) and the ulna (UI). The distal autopod (A, in red) forms the wrist bones, the palm bones and the digits. Red and blue histological stains mark ossified bone and cartilage, respectively. The antero-posterior and the proximo-distal axis are depicted above.

Adapted from Bénazet and Zeller, 2009 and Zeller and Zuniga, 2007

## I.2. Anteroposterior growth and patterning of the limb bud

In vertebrates, the antero-posterior (AP) growth and patterning of the limb bud is coordinated by a small posterior mesenchymal region called the zone of polarizing activity (ZPA), which is considered the posterior organizer of the limb bud due to its potential to instruct cells with respect to their AP fates (Robert and Lallemand, 2006; Zeller *et al.*, 2009). Grafting experiments in chick have shown that anterior ectopic grafts of ZPA cells are able to induce mirror-image digit duplications along the AP axis, which at first sight, can apparently be explained by the French-flag model formulated by Wolpert in 1969 (Wolpert, 1969) (Fig.3). This model postulated that ZPA cells produce a morphogen signal whose diffusion establishes a spatial gradient across the limb bud,

with its highest concentration in the posterior mesenchymal region corresponding to the ZPA. In response, mesenchymal cell fates were specified according to three distinct threshold values of the morphogen (depicted in the model by the three colors of the French flag), depending on their distance from the source (Zeller, 2004; Zeller *et al.*, 2009).

After twenty years of intensive searching for the long-lost Wolpert's morphogen, a small diffusible protein called Sonic Hedgehog (SHH) was identified as the morphogen signal produced by the ZPA (Riddle *et al.*, 1993). After being secreted by the ZPA, the SHH protein diffuses across the limb bud to elicit responses at a distance in

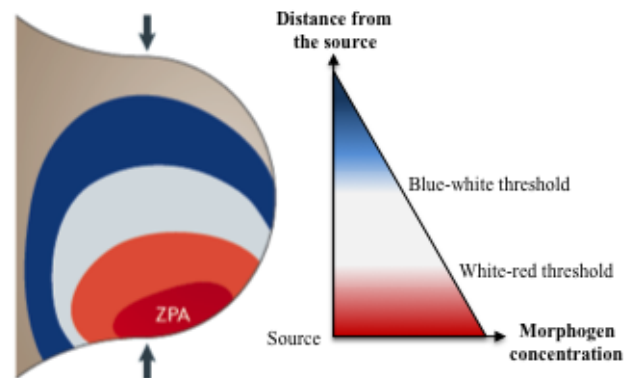


**Figure 3 The French-flag model proposed by Wolpert.** The ZPA in the posterior limb bud mesenchyme is indicated in red and corresponds to the highest point of the SHH morphogenetic gradient established across the entire limb bud. The identities of the limb bud mesenchymal cells are specified by threshold levels of the morphogen, depicted in the model by the three colors of the French flag.

**Adapted from Zeller *et al.*, 2009**

the mesenchyme, as suggested by grafting experiments showing that *Shh*-expressing fibroblasts are able to induce mirror-image digit duplications when placed anteriorly in the limb bud mesenchyme (Lewis *et al.*, 2001). Furthermore, genetic experiments have revealed that the lack of *Shh* during limb bud morphogenesis resulted in the loss of posterior limb structures, including the ulna and digits 5 to 2, thus proving the absolute requirement of *Shh* signaling for the AP growth and patterning of the vertebrate limb (Chiang *et al.*, 2001; Kraus *et al.*, 2001). Although most studies converge on the existence of a spatial morphogen gradient, none has analyzed the kinetics of SHH gradient formation and the postulated threshold responses, nor the direct contribution of ZPA cells to digit primordia. To address these issues, a series of experiments were devised in order to label all *Shh*-expressing cells and follow their descendants throughout time during limb development (Ahn and Joyner, 2004; Harfe *et al.*, 2004). These cell lineage tracing experiments revealed that *Shh* descendant cell populations give rise to posterior digits (from digit 5 to 3), whereas digit 2 is the only skeletal element whose specification is entirely dependent on long-range SHH signaling (Fig.4A). These results challenged the relevance of the spatial morphogen gradient

proposed earlier by Lewis Wolpert and, together with other studies, contributed to the establishment of a new model postulating that mesenchymal cells are able to acquire a kinetic memory of the SHH signal they have received and subsequently respond according to the exposure time length (*i.e.* the posterior cells exposed to SHH the longest are fated to become digit 5, whereas anterior cells never exposed to SHH are fated to become digit 1) (Zeller, 2004).

### I.3. The Shh/Gli3/Msx regulatory genetic network

At the molecular level, the main role of Shh during limb development is to counteract the activity of the transcription factor Gli3 by preventing the formation of Gli3R, a truncated form of the Gli3 protein that acts as a transcriptional repressor (Wang *et al.*, 2000). To fulfill its function, Shh signaling acts at two distinct levels: first it represses *Gli3* transcription in a dose-dependent manner, such that *Gli3* mRNA is transcribed according to a gradient opposite to Shh which increases from the anterior to the posterior region of the limb bud (Fig.4).

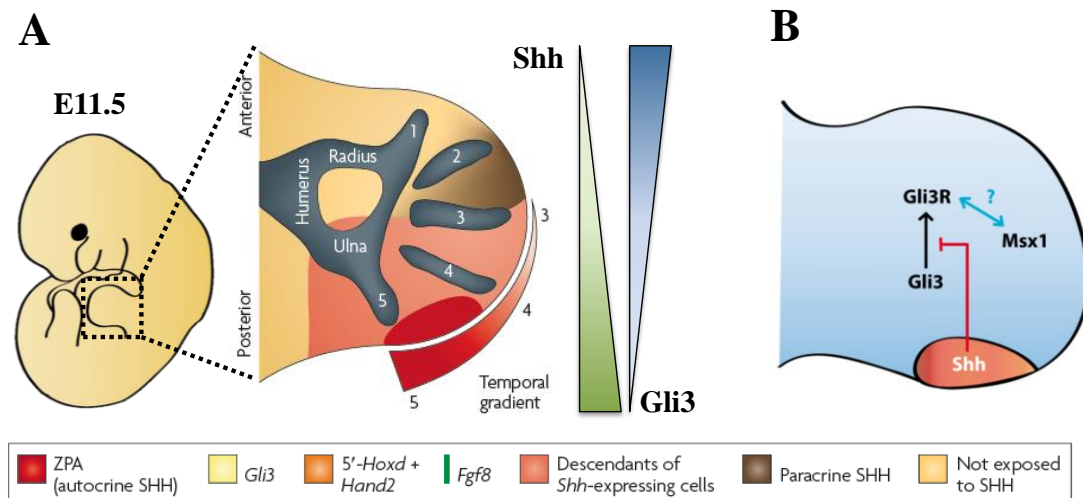


**Figure 4** The Shh/Gli3/Msx regulatory genetic network controls the antero-posterior pre-patterning of the limb bud. (A) Specification of anteroposterior identities by a spatial and temporal gradient of Shh and Gli3. Descendants from Shh-expressing cells give rise to digits 4 and 5, and contribute to digit 3. Cells that give rise to digit 2 and parts of digit 3 are specified by long-range SHH signaling. The digit 1 is specified in a SHH-independent manner. The transcriptional repression of Gli3 by Shh signaling is responsible for the establishment of a Gli3 gradient from posterior to anterior. (B) The involvement of Msx within the Shh/Gli3 genetic network. A set of evidences suggest that the transcription factor Msx1 may be involved in this genetic network by interacting with Gli3R, the repressor form of the transcription factor Gli3.

Adapted from Zeller *et al.*, 2009



Second, it is required to prevent the processing of Gli3 into its repressor form, Gli3R, which accumulates primarily in cells that do not express Shh. These genetic interactions result in the pre-patterning of the nascent limb bud, defining two clearly distinct regions: the anterior limb bud containing high levels of Gli3R and low Gli3A levels, and the converse in the posterior region close to the Shh signaling domain (Wang *et al.*, 2000; Zeller *et al.*, 2009). Nevertheless, while the mechanism allowing Shh to modulate Gli3 activity is well documented, the role of other genes important for AP patterning within this regulatory genetic network remains poorly understood. Due to their involvement in AP limb patterning, Msx genes, which constitute a small family of genes encoding homeodomain transcription factors, are considered good candidates for interacting within this genetic loop (Lallemand *et al.*, 2009; Bensoussan *et al.*, 2011). In the mouse, the Msx family comprises three members, two of which, Msx1 and Msx2, were proposed to play a role in limb development as both are expressed from the onset of limb bud outgrowth in the ectoderm and mesoderm as well (Davidson *et al.*, 1991; Robert *et al.*, 1991) (Fig.5 and Fig.S.1). Due to the high level of functional redundancy between these two genes, neither *Msx1* nor *Msx2* null mutants display limb abnormalities. However, *Msx1*<sup>-/-</sup>; *Msx2*<sup>-/-</sup> double homozygous mutants exhibit several malformations along the AP axis, including the loss of anterior autopod and zeugopod structures and, later on, the abnormal overgrowth of the remaining anterior part of the autopod mesenchyme (Lallemand *et al.*, 2005).

Several lines of evidence suggest that Msx genes may play a crucial role in limb morphogenesis by interacting with the transcription factor Gli3, and in particular with its repressor form, Gli3R (Fig.4B). First, Lallemand and co-

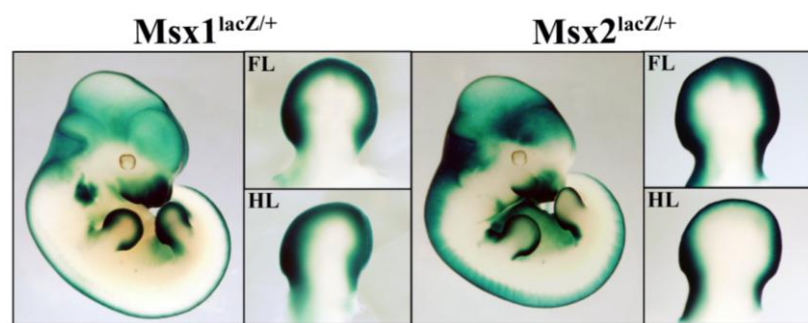


**Figure 5 Expression pattern of Msx1 and Msx2 visualized in whole-mount at E11.5, using the lacZ reporter.** Both Msx1 (left panel) and Msx2 (right panel) are highly expressed in the distal region of the limb bud, in the central nervous system and in the olfactory bulb. The forelimb (FL) and hindlimb (HL) of each embryo are shown beside each panel.

workers have demonstrated that at E11.5 there is an overlapping expression domain of Msx1 and Gli3, corresponding to the most anterior region of the limb bud (presumptive



territory of digit 1), where both genes are expressed at a high level. This spatial and temporal co-localization suggested that these two transcription factors might share similar functions during limb bud development, which was supported by results showing that in the absence of *Msx* genes and/or *Gli3*, the limb bud anterior apoptotic domain normally observed at E11.5 was absent, suggesting that both genes are required for apoptosis of anterior tissues in the limb at this specific time point (Aoto *et al.*, 2002; Lallemand *et al.*, 2009). Furthermore, in *Msx* and *Gli3* mutants, anterior and posterior identity markers have their expression similarly affected, *i.e.*, the anteriorly restricted *Pax9* is downregulated in *Gli3*<sup>-/-</sup> and *Msx1*<sup>-/-</sup>; *Msx2*<sup>+/-</sup>, whereas the posterior marker *Hand2* expands anteriorly in both cases (Y. Lallemand and B. Robert, unpublished data; Bowers *et al.*, 2012). In an effort to address the role of *Msx* genes within the *Shh*/*Gli3* regulatory genetic network and investigate possible epistatic interactions, Lallemand *et al.* have created a series of *Shh* and *Msx* compound mutants and analyzed their phenotypes. In a *Shh*<sup>-/-</sup> null mutant background where *Gli3R* is overproduced, all digits but digit one are lost because of extensive apoptosis of the mesenchyme (te Welscher *et al.* 2002). In this genetic context, limb skeletal analyses have demonstrated that when *Msx* genes are also mutated, digit formation was partially restored because apoptosis is prevented in the domain where *Msx* are normally expressed. Interestingly, te Welscher *et al.* (2002) and Litingtung Litingtung *et al.* (2002) had previously shown that a similar phenotype rescue is observed when functional *Gli3* alleles are removed in a *Shh*<sup>-/-</sup> null mutant background. Taken together, these results demonstrate that both *Msx1* and *Gli3* are epistatic over *Shh* and suggest, once again, that both transcription factors play identical roles during limb development and might, possibly, interact with each other. Finally, the most direct evidence pointing to an interaction between these two genes was provided by a Co-IP experiment performed in the lab using an *in vitro* system where HEK293 cells were co-transfected with cDNAs encoding tagged forms of *Msx1* (*Msx1*<sup>C-myc</sup>) and *Gli3R* (*Gli3R*<sup>Flag</sup>). The Western Blot results have revealed that it was possible to cross-precipitate both *GLI3R* and *MSX1* proteins using antibodies raised against the C-myc and the Flag tag of *Msx1* and *Gli3R*, respectively, indicating that these two proteins are able to interact with each other under these experimental conditions (O. Goupille and B. Robert, unpublished data) (Fig.6). However, it is important to highlight the fact that the expression level of these proteins is not controlled in these experiments and thus might not reflect what happens *in vivo* in the

limb bud. In order to solve this issue, it is imperative to establish a proper *in vivo* system that allows the study of genetic interactions taking place during limb bud development, which is the main goal of the present work.

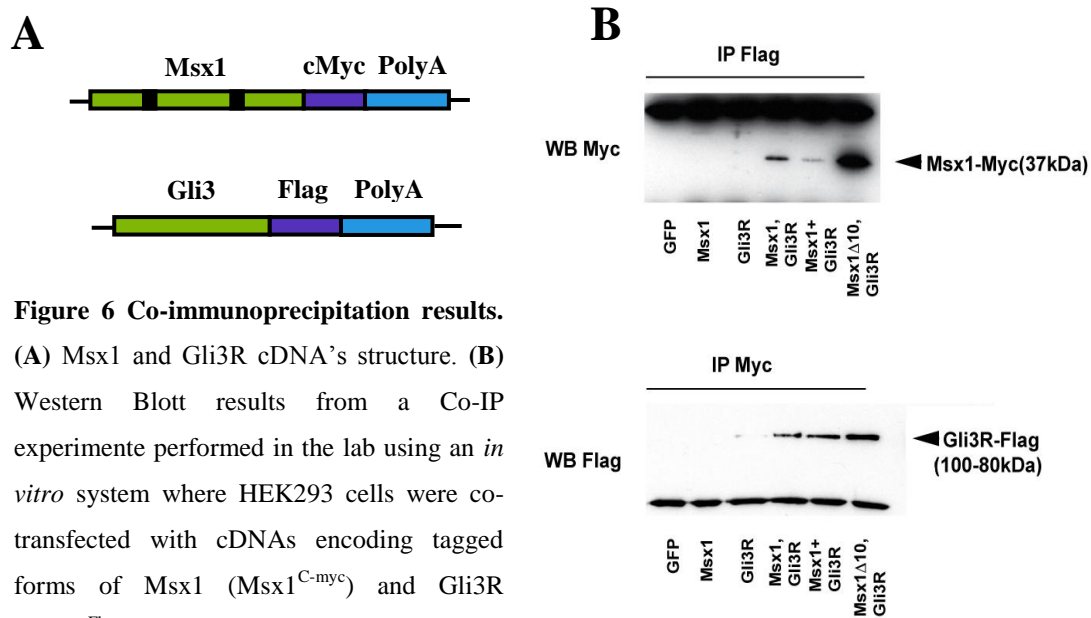


**Figure 6 Co-immunoprecipitation results.**

(A) Msx1 and Gli3R cDNA's structure. (B)

Western Blott results from a Co-IP experiment performed in the lab using an *in vitro* system where HEK293 cells were co-transfected with cDNAs encoding tagged forms of Msx1 (Msx1<sup>C-myc</sup>) and Gli3R (Gli3R<sup>Flag</sup>) have revealed that it is possible to

cross-precipitate both MSX1 and GLI3R proteins using antibodies against the Flag and the C-myc tag of Gli3R and Msx1, respectively (top and bottom panel, respectively).

Courtesy of Benoît Robert, Dr.

## I.4. The involvement of Msx1 and Gli3R in the BMP signaling pathway

Previous studies addressing palate formation in the mouse have demonstrated that embryos lacking *Bmpr1A* or *Msx1* developed a cleft palate, a craniofacial malformation where the two palatal shelves are not completely joined to form the hard palate (Liu *et al.*, 2005; Zhang *et al.*, 2002). Surprisingly, transgenic mice harboring the human *Bmp4* gene driven specifically in the craniofacial region by the mouse *Msx1* promoter on an *Msx1*<sup>-/-</sup> null mutant background displayed palatal closure, suggesting that Msx genes are interacting with the BMP signaling pathway in order to drive palate formation (Zhang *et al.*, 2002). Nevertheless, other studies have demonstrated that the phosphorylation of the Bmp receptor following ligand binding is not compromised in *Msx1*; *Msx2* deficient mice, indicating that Msx1 is acting at a different level in the BMP signaling cascade (Liu *et al.*, 2005; Ovchinnikov *et al.*, 2006). Interestingly, the finding that Gli2 and Gli3 are expressed in close proximity to many sites of active BMP signaling (Lee *et al.*, 1997), together with the observation that many Human syndromes arising from

mutations that produce truncated Gli3 proteins result in defects reminiscent of those caused by BMP signaling impairment (Kang *et al.*, 1997), raised the possibility that these Gli proteins may also interact with the BMP cascade and that this might occur via the Smad proteins, which constitute the intracellular transducers of the TGF $\beta$  family members, including BMP's. In the BMP signaling cascade, the Smad1,5,8 protein complex becomes phosphorylated following ligand binding to their receptor. These, after associating with Smad4, translocate into the nucleus where they will bind to specific DNA domains and promote the transcription of BMP target genes, thus constituting the active transcription factors in the BMP pathway (Kimelman, 2006). By taking advantage of an *in vitro* system where COS1 cells were transfected either with full-length or truncated forms of Gli3, Liu *et al.* (1998) were able to demonstrate that only carboxy-terminally truncated Gli3 proteins (structurally similar to the Gli3R transcriptional repressor) were able to associate with endogenous Smads through their zinc finger domain. Taken together these results prompted us to investigate, in a more detailed manner, the involvement of Msx1 and Gli3R in the BMP signaling pathway, by testing whether these proteins are able to bind and interact with the PSmad1,5,8 protein complex, thus modulating its transcriptional activity over BMP target genes.

## II. Objectives

Although a significant amount of indirect evidences point to the existence of genetic interactions between the transcription factors Msx1 and Gli3R, it remains to be demonstrated whether direct interactions between these corresponding proteins can be demonstrated at the *in vivo* level. Thus, the main goal of this project is to establish a proper *in vivo* system that allows the study of endogenous protein interactions taking place during mouse limb bud development. To this end, we aim to:

1. Raise transgenic mice lines harboring constructs that will allow for the *in vivo* detection of Msx1 and Gli3R and test their efficiency;
2. Untangle the relationship between Msx1 and Gli3R using the mouse limb bud at 11.5 *dpc* as a model system;
3. Investigate the involvement of Msx1 and Gli3R in the BMP signaling cascade via the PSmad1,5,8 protein complex

### III. Materials and Methods

#### III.1. Mouse strains and genotyping

In order to study the potential endogenous interactions between *Msx1* and Gli3R we have used a transgenic mouse line harboring a Cre-inducible Gli3 repressor containing a flag sequence inserted into the *Rosa26* locus (Vokes *et al.*, 2008), together with a floxed Gli3 allele (Blaess *et al.*, 2008) and a non-inducible tagged form of the *Msx1* gene (N. Duval and B. Robert, unpublished data) (Fig.7). By crossing homozygous males belonging to the murine line carrying these transgenes with homozygous females harboring the Cre recombinase driven by the *Prx1* limb enhancer (Logan *et al.*, 2002), it

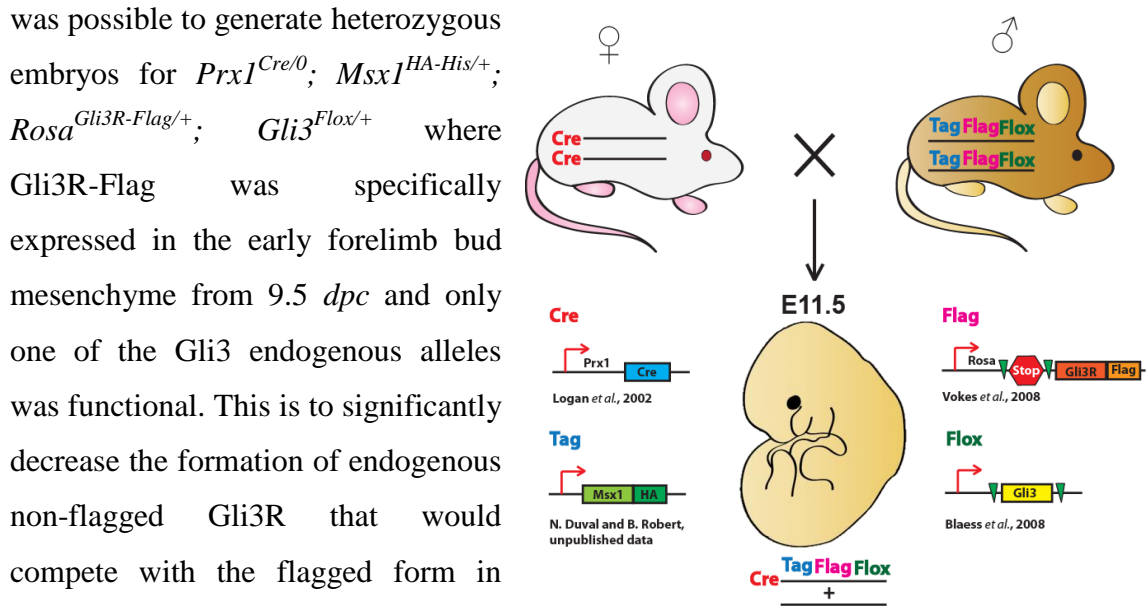


**Figure 7** Mating strategy adopted to generate heterozygous embryos for *Prx1*<sup>Cre/0</sup>; *Msx1*<sup>HA-His/+</sup>; *Rosa*<sup>Gli3R-Flag/+</sup>; *Gli3*<sup>Flox/+</sup>. The structure of the transgenes present in the animals are shown on both sides of the panel.

transgene when transmitted maternally. According to Logan *et al.* (2002), in this case germline recombination might occur in the offspring, resulting in the expression of Cre outside the limb field from the very first stages of development. The penetrance of this germline recombination event relied also on the particular strain and gene that ought to be defloxed. This potential loss of tissue and stage specificity raised a problem and prompted us to analyze the Cre recombinase activity in E11.5 embryos using the

*Rosa<sup>nlacZ</sup>* reporter before proceeding with our experiments. The analysis of the expression pattern revealed that by E11.5, Cre activity was restricted to the limb bud mesenchyme and absent both in the AER and ectoderm, thus validating the use of this transgenic line for our experiments (Fig.8). All embryos were then collected on the 11<sup>th</sup> day following plug observation, corresponding to the stage where both *Msx1* and *Gli3R* reach their highest expression level. The day of the plug was considered as 0.5 *dpc*. Genotyping of the *Msx1<sup>HA-His</sup>*, *Rosa<sup>Gli3R-Flag</sup>* and *Gli3<sup>Flox</sup>* alleles was performed by PCR following the protocol summarized in Table 1. Control embryos harboring only either *Msx1<sup>HA-His</sup>* or *Rosa<sup>Gli3R-Flag</sup>* were selected among the littermates of *Prx1<sup>Cre/0</sup>*; *Msx1<sup>HA-His/+</sup>*; *Rosa<sup>Gli3R-Flag/+</sup>*; *Gli3<sup>Flox/+</sup>* embryos.

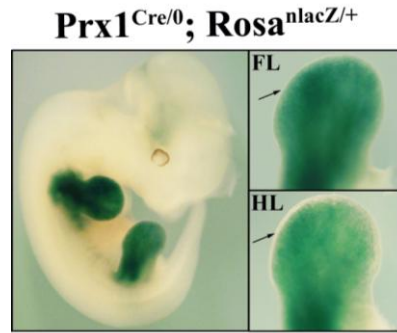


**Figure 8 Cre recombinase activity visualized in whole-mount at E11.5, using the lacZ reporter.** Cre recombinase activity is detected in *Prx1-Cre* mice using the *Rosa<sup>nlacZ</sup>* reporter in the forelimb and hindlimb mesenchyme but not in the ectoderm (black arrows). The forelimb (FL) and hindlimb (HL) of each embryo are shown beside each panel.

**Table 1. PCR protocol.**

PCR		
1.	DNA extraction	1. Centrifuge tail/digit samples for 6 sec to ensure that the tissue is at the bottom of the tube 2. Add 50 $\mu$ L of the PCR extraction solution to each tube containing the samples
2.	DNA denaturation	1. Place the tubes at the heating machine for 20 min at 99°C
3.	Preparation of the PCR cocktail	1. Add water, loading buffer, reaction buffer, $MgCl_2$ , Oligos, dNTPs and Taq polymerase <sup>1</sup> (for one reaction of 24 $\mu$ L, add: 18,50 $\mu$ L distilled water, 2,5 $\mu$ L loading buffer, 2,5 $\mu$ L reaction buffer, 0,75 $\mu$ L 50 mM $MgCl_2$ , 0,5 $\mu$ L 10 $\mu$ M primer mix, 0,2 $\mu$ L 25mM dNTPs and 0,1 $\mu$ L Taq polymerase)
4.	DNA neutralization	1. Remove the tubes from the heating machine and centrifuge them again for 1 min 2. Add 50 $\mu$ L of neutralization buffer to each tube containing the samples 3. Centrifuge the sample tubes again for 1 min
5.	Preparation of the PCR tubes	1. Aliquot 24 $\mu$ L of the PCR mixture into small PCR tubes 2. Add 1 $\mu$ L of each DNA sample to the aliquots containing the PCR mixture 3. Place the caps on the tubes and close them firmly
6.	PCR reaction	1. Choose the program <sup>2</sup> and place the aliquots into the PCR machine
7.	Gel preparation	1. Place the combs and the borders into the plastic support 2. Pour between 35 and 40 mL of the gel mixture containing one drop of ethidium bromide 3. Add some TBE on top of the gel to cover it completely
8.	Running the gel	1. Pipette 12 $\mu$ L of each PCR aliquot into each well 2. Run the gel for 15 min at 135V
9.	Gel revelation	1. Place the gel in the UV machine to acquire photos

<sup>1</sup> The quantities of each reagent should be adjusted to the number of reactions

<sup>2</sup> 35 cycles for *Msx1<sup>HA-His</sup>* and *Gli3<sup>Flox</sup>* and 40 cycles for *Rosa<sup>Gli3R-Flag</sup>*

### **III.2. LacZ staining**

Embryos from E11.5 up to E13.5 were dissected in PBS 1X and fixed in 4% PFA at 4°C for one hour. After being washed three times in PBS 1X, these embryos were placed in a solution containing the enzyme  $\beta$ -galactosidase (see [Appendix II](#) for a complete list of the solutions and buffers used in the experiments) and then incubated at 4°C overnight under slight agitation in the absence of light. On the next day, the embryos were washed three times in PBS 1X in order to stop the reaction and photographed under the binocular stereoscopic microscope.

### **III.3. Alcian Blue cartilage staining**

Embryos from E13.5 up to E15.5 were dissected in PBS 1X and fixed in 4% PFA at 4°C overnight. After being washed three times in PBS 1X, these embryos were refixed in 80% Ethanol overnight at 4°C. On the following day, the embryos were placed in a staining solution containing Alcian Blue (see [Appendix II](#)) and kept for one day at 4°C under slight agitation. Afterwards, they were washed twice in 80% Ethanol-20% Acetic acid and kept overnight at 4°C. On the following day we proceeded to the visualization step by washing the embryos twice in 70% Ethanol-1% HCl solution keeping them again overnight at 4°C. On the last day, the embryos were placed in 1% NaOH for 5-10 min to clear the skin and reveal the cartilage blue staining, washed twice in PBS 1X and photographed under the binocular stereoscopic microscope.

### **III.4. Alizarin Red skeletal staining**

4-day old pups (P4) were euthanized by asphyxia with dry ice, eviscerated and then boiled at 70°C for 20 min. After removing the skin, the newborns were fixed in 70% Ethanol overnight at 4°C. On the following day, they were transferred into 1% NaOH and kept for one day to allow soft tissue dissociation. Afterwards the solution was replaced by adding fresh 1% NaOH together with 2 mL of Alizarin Red (see [Appendix II](#)) and the newborns were kept in for 1-2 days at 4°C without agitation. To clear the skeleton, the newborns were then kept in 0,01% NaOH for several days. After removing all the unspecific red staining, they were washed twice in PBS 1X and photographed under the binocular stereoscopic microscope.

### III.5. Limb bud protein extraction

For protein extraction of endogenous MSX1 and GLI3R proteins, both forelimbs and hindlimbs from E11.5 embryos were dissected in PBS 1X and placed on an *eppendorf* tube containing 20  $\mu$ L of Lysis Buffer (20  $\mu$ L of Lysis Buffer/limb bud) (see [Appendix II](#)). Afterwards, the limbs were repeatedly pipetted with a 200  $\mu$ L pipette in order to improve tissue dissociation. The entire extraction procedure was performed on ice to avoid protein degradation. Following the extraction procedure, the limb bud lysates were then centrifuged for 30 min at 13 000 rpm at 4°C and the supernatants were recovered and stored at -80°C until further use.

### III.6. Co-Immunoprecipitation (Co-IP) and Western Blotting

For Co-IP of endogenous MSX1 and GLI3R embryonic proteins, primary antibodies raised against the HA tag of Msx1 (Anti-HA Sigma Aldrich, ref: H6908) and the Flag tag of Gli3R (Anti-Flag Sigma Aldrich, ref: F1804) were covalently linked to magnetic Dynabeads® as described in the product protocol summarized in [Table 2](#). Afterwards, the beads and limb bud lysates from E11.5 embryos were mixed and incubated with tilting and rotation. The Dynabeads®-Ab-Antigen bound complex was then eluted for direct downstream analysis by Western blotting, following the protocol summarized in [Table 3](#). After being separated by SDS-PAGE electrophoresis, the proteins from the lysates were transferred onto a nitrocellulose membrane. The membranes were then washed in blocking buffer solution, incubated with primary and secondary antibodies and imaged by chemiluminescence. Controls included a negative control where the protein extract was not associated with the antibody (-Ab), an input (positive control) corresponding to the pure limb bud extract, the IPs for each individual protein to guarantee that they were present in the limb extract, and finally the Co-IP.

### III.7. Proximity Ligation Assay (PLA)

The PLA assay allows the *in situ* visualization of protein-protein interactions within cells using primary antibodies directed against specific proteins together with oligonucleotide-conjugated secondary antibodies. The principle is that when the PLA secondary probes are in close proximity (*i.e.* when two proteins are interacting with



each other), the DNA strands can interact and form a dsDNA loop. After joining of the two oligonucleotides by enzymatic ligation, they are amplified via rolling circle amplification using a polymerase. Following the DNA amplification reaction, fluorescent-labeled complementary oligonucleotide probes highlight the reaction site as a distinct bright dot when viewed under the fluorescence microscope (Fig.9).

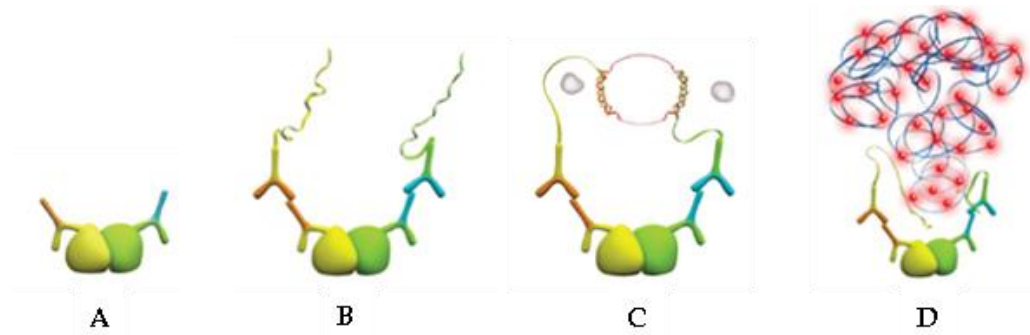


**Figure 9 Principle of the PLA.** **A.** Primary antibodies bind to their respective proteins. **B.** Duolink PLUS and MINUS secondary antibodies bind to the primary antibodies. **C.** When the PLUS and MINUS probes are in close proximity (less than 40 nm), the ssDNA reach each other and, with the Duolink Ligase solution, the strands form a dsDNA loop. **D.** After amplification, fluorescent probes bind to the complementary oligonucleotide sequence and the reaction site can be visualized under a fluorescence microscope.

**Adapted from the Duolink *In Situ* User Fluorescence User Manual**

In order to investigate possible interactions between MSX1, GLI3R and the PSmad1,5,8 protein complex, E11.5  $Prx1^{Cre/0}$ ;  $Msx1^{HA-His/+}$ ;  $Rosa^{Gli3R-Flag/+}$ ;  $Gli3^{Flox/+}$  and  $Prx1^{Cre/0}$ ;  $Msx1^{HA-His/+}$  control embryos were dissected in PBS 1X and fixed in 4% PFA at 4°C overnight. On the next day after being washed three times in PBS 1X, these embryos were embedded using Tissue Freezing Medium. The blocks containing the embryos were stored at -20°C until they were sectioned transversally at the cryostat (sections with 12 µm of thickness). Afterwards, the sections were washed in PBS 1X to remove the freezing medium, blocked and incubated with the primary antibodies (see [Appendix III](#) for a complete list of the antibodies used in the experiments) at 4°C overnight. The following steps were performed using the Duolink *In Situ* Orange Starter Kit, according to the manufacturer protocol summarized in [Table 4](#). Sections of the forelimbs, hindlimbs and neural tube were then photographed using the 63x objective of the Zeiss LSM700 confocal microscope with the DAPI ( $\lambda=358$  nm) and Cy3 ( $\lambda=550$  nm) filters. The pictures taken were then analyzed using Adobe Photoshop CS5, ImageJ and Icy.

**Table 2. Immunoprecipitation protocol using Dynabeads®.**

<b>Immunoprecipitation using Dynabeads®</b>		
<b>1.</b>	<b>Washing</b>	<ol style="list-style-type: none"> <li>1. Resuspend Dynabeads® thoroughly by vortexing 1-2 min</li> <li>2. Transfer 50 µL of Dynabeads® to a tube, place on the magnet and remove the supernatant</li> <li>3. Remove the tube from the magnet and resuspend the Dynabeads® in 500 µL of 0.1 M Na-acetate pH 5</li> <li>4. Place the tube on the magnet and remove the supernatant</li> <li>5. Repeat steps 3 and 4 twice</li> </ol>
<b>2.</b>	<b>Ig capture</b>	<ol style="list-style-type: none"> <li>1. Dilute 1 µL of Anti-HA or Anti-Flag in 100 µL of PBS-0,1% Tween-20 and add it to the solution containing the washed Dynabeads®</li> <li>2. Incubate with slow tilting and rotation for 1h at RT</li> <li>3. Place the test tube on the magnet for 2 min and pipette off the supernatant</li> <li>4. Remove the tube from the magnet and resuspend the Dynabeads® in 500 µL of 0.1 M Na-acetate pH 5</li> <li>5. Place the tube on the magnet and remove the supernatant</li> <li>6. Repeat steps 3 and 4 twice</li> </ol>
<b>3.</b>	<b>Crosslinking</b>	<ol style="list-style-type: none"> <li>1. Wash the Dynabeads®-Ig complex in 1 mL of 0.2 M triethanolamine, pH 8.2 for 5 min, with the use of the magnet</li> <li>2. Resuspend the Dynabeads®-Ig complex in 1 mL of freshly made 20 mM DMP in 0.2M triethanolamine, pH 8.2</li> <li>3. Incubate with gentle mixing for 30 min at 20°C. Place the tube on the magnet and discard the supernatant.</li> <li>4. Remove the tube from the magnet and stop the reaction by resuspending the Dynabeads® - Ig complex in 1 ml of 50 mM Tris, pH 7.5</li> <li>5. Incubate for 15 min with gentle mixing at RT</li> <li>6. Wash the Dynabeads® - Ig complex 1 time with 100 µL of PBS-0,1% Tween-20</li> </ol>
<b>4.</b>	<b>Antigen binding</b>	<ol style="list-style-type: none"> <li>1. Add 200 µL of the sample containing antigen directly to the Dynabeads® - Ig complex</li> <li>2. Incubate overnight with slow tilting and rotation at 4°C</li> <li>3. Place the tube on the magnet and discard the supernatant</li> <li>4. Wash the Dynabeads® on the following day three times with 1mL of PBS 1X</li> <li>5. Place the tube on the magnet and remove the supernatant</li> </ol>
<b>5.</b>	<b>Elution</b>	<ol style="list-style-type: none"> <li>1. Prepare 20 µL of Laemlli-5%β-mercaptoethanol and mix with 20 µL of 0.1M Citrate, pH 2</li> <li>2. Add the mixture to the Dynabeads®-Ig-Ag complex and incubate for 10 min at 70°C</li> <li>3. Place the tube on the magnet and remove the supernatant</li> <li>4. Load the supernatant directly onto a gel for downstream analysis</li> </ol>

### III.8. Immunofluorescence

Embryos were dissected in PBS 1X and fixed in 4% PFA at 4°C overnight. On the next day after being washed three times in PBS 1X, both forelimbs and hindlimbs were dissected in PBS 1X and embedded using Tissue Freezing Medium. The blocks containing the limb buds were stored at -20°C until they were sectioned transversally at the cryostat (sections with 12 µm of thickness). Afterwards, an immunodetection against Caspase3 (see [Appendix III](#)) was performed on the transverse sections obtained in order to analyse the apoptosis taking place in the limb bud in the normal and *Msx1*<sup>-/-</sup>; *Msx2*<sup>-/-</sup>

**Table 3 Western Blotting protocol.**

<b>Western Blotting</b>		
<b>1. Running the gel</b>		<ol style="list-style-type: none"> <li>1. Load the samples onto the gel and run it for 1h at 150V</li> <li>2. Remove the gel from the apparatus</li> </ol>
<b>2. Transferring</b>		<ol style="list-style-type: none"> <li>1. Prepare the sandwich for transferring, by placing Whatman paper, nitrocellulose membrane, the equilibrated gel and Whatman paper soaked in transfer buffer onto the Trans-Blot SD semi-dry cell</li> <li>2. Roll a pipette over the sandwich to remove bubbles</li> <li>3. Run for 30 min at 10V</li> </ol>
<b>3. Blocking</b>		<ol style="list-style-type: none"> <li>1. Place the nitrocellulose membrane in TBS-5% milk-0,1% Tween-20 and incubate for 1h at RT under gentle agitation</li> </ol>
<b>4. 1<sup>st</sup> Antibodies</b>		<ol style="list-style-type: none"> <li>1. Dilute the primary antibodies (Anti-HA or Anti-Flag 1:1000) in TBS-5% milk-0,1% Tween-20 and incubate overnight at 4°C</li> <li>2. Wash 5 times 5 min in TBS-0,1% Tween-20 under gentle agitation at RT</li> </ol>
<b>5. 2<sup>nd</sup> Antibodies</b>		<ol style="list-style-type: none"> <li>1. Dilute the secondary antibodies (Anti-rabbit or Anti-mouse HRP-conjugated 1:10000) in TBS-5% milk-0,1% Tween-20 and incubate for 1h at RT</li> <li>2. Wash 5 times 5 min in TBS-0,1% Tween-20 under gentle agitation at RT</li> </ol>
<b>6. Revelation</b>		<ol style="list-style-type: none"> <li>1. Place the nitrocellulose membrane onto Saran wrap paper and transfer it to an X-ray cassette</li> <li>2. Mix 250 µL of the two reagents provided in the Super Signal West Pico Chemiluminescent Substrate and apply it directly over the nitrocellulose membrane</li> <li>3. Reveal by exposing the Hyper Film ECL from 1-5 min</li> </ol>

**Table 4 Proximity Ligation Assay protocol.**

<b>Proximity Ligation Assay</b>		
<b>1. Blocking</b>		<ol style="list-style-type: none"> <li>1. Add blocking solution to the slides. Incubate for 1h at 37°C.</li> <li>2. Remove the blocking solution</li> </ol>
<b>2. Primary antibodies</b>		<ol style="list-style-type: none"> <li>1. Dilute the primary antibodies in the Antibody Diluent solution provided in the Kit and incubate overnight at 4°C in a humidity chamber (Anti-mouse 1:50 and Anti-rabbit 1:500)</li> <li>2. Wash in 1X Wash Buffer A 2 times 5 min</li> </ol>
<b>3. PLA<sup>®</sup> probes</b>		<ol style="list-style-type: none"> <li>1. Dilute the MINUS and PLUS probes 1:5 in the Antibody Diluent solution and apply it to the slides</li> <li>2. Incubate in a pre-heated humidity chamber for 60 min at 37°C</li> <li>3. Wash in 1X Wash Buffer A 2 times 5 min</li> </ol>
<b>4. Ligation</b>		<ol style="list-style-type: none"> <li>1. Dilute the Ligation stock 1:5 in H<sub>2</sub>O</li> <li>2. Add Ligase to the Ligation solution at a 1:40 dilution and vortex</li> <li>3. Add the Ligation-Ligase solution to each slide</li> <li>4. Incubate in a pre-heated humidity chamber for 30 min at 37°C</li> <li>5. Wash in 1X Wash Buffer A 2 times 2 min</li> </ol>
<b>5. Amplification</b>		<ol style="list-style-type: none"> <li>1. Dilute the Amplification stock 1:5 in H<sub>2</sub>O</li> <li>2. Add Polymerase to the Amplification solution at a 1:80 dilution and vortex</li> <li>3. Add the Amplification-Polymerase solution to each slide</li> <li>4. Incubate in a pre-heated humidity chamber for 100 min at 37°C</li> <li>5. Wash in 1X Wash Buffer B 2 times 10 min</li> <li>6. Wash in 0,01X Wash Buffer B for 1min</li> <li>7. Let the slides dry at RT in the dark</li> </ol>
<b>6. Imaging</b>		<ol style="list-style-type: none"> <li>1. Mount the slides with Duolink <i>In Situ</i> Mounting Medium with DAPI</li> <li>2. Wait 15 min before visualizing in a fluorescence or confocal microscope or store the slides at -20°C</li> </ol>

mutant background, respectively. The protocol followed is summarized in Table 5. Sections of the forelimbs and hindlimbs were then photographed using the 63x objective of the Zeiss LSM700 confocal microscope with the Alexa Fluor 488 ( $\lambda=495$  nm) and the DAPI ( $\lambda=358$  nm) filters. The pictures taken were then analyzed using Adobe Photoshop CS5 and ImageJ.

**Table 5 Immunofluorescence protocol.**

<b>Immunofluorescence on sections</b>		
<b>1.</b>	<b>Freezing medium removal</b>	<b>1.</b> Wash in PBS 1X, 2 times 5 min at RT
<b>2.</b>	<b>Permeabilization</b>	<b>1.</b> Wash in PBS-0,2% TritonX-100 for 20 min at RT
<b>3.</b>	<b>Blocking</b>	<b>1.</b> Block in PBS-1% BSA-5% GS-0,5% Triton X100 for 1h at RT
<b>4.</b>	<b>Primary antibodies</b>	<b>1.</b> Dilute the antibodies in PBS-1% BSA-5% GS-0,5% Triton X100 and incubate overnight at 4°C in a humidity chamber
<b>5.</b>	<b>Washes</b>	<b>1.</b> Wash in PBS 1X, 3 times 10 min at RT
<b>6.</b>	<b>Secondary antibodies</b>	<b>1.</b> Dilute the antibodies in PBS-1% BSA-5% GS-0,5% Triton X100 and incubate for 1h at RT in a humidity chamber in the absence of light
<b>7.</b>	<b>Washes</b>	<b>1.</b> Wash in PBS 1X, 1 time 10 min at RT, in the absence of light
<b>8.</b>	<b>Hoechst staining</b>	<b>1.</b> Dilute Hoechst in PBS 1X (1:2000) <b>2.</b> Incubate for 5 min at RT in the absence of light
<b>9.</b>	<b>Washes</b>	<b>1.</b> Wash in PBS 1X, 2 times 10 min at RT, in the absence of light
<b>10.</b>	<b>Dako Mounting</b>	<b>1.</b> Place 2 or 3 drops of Dako mounting medium on top of the slide <b>2.</b> Place the coverslip on top of the slide by using fine forceps, carefully to avoid air bubbles
<b>11.</b>	<b>Storage &amp; Observation</b>	<b>1.</b> Store the slides at -20°C in the absence of light <b>2.</b> Observe the sections at the fluorescence or confocal microscope

### III.9. Statistical analysis

For the PLA, the area (in  $\text{mm}^2$ ) and fluorescence observed on the transverse sections of the forelimb, hindlimb and neural tube were determined using the Spot Detector plugin of the Icy software. The fluorescence density of each section was then calculated by the quotient between the number of fluorescent dots detected and the area in  $\text{mm}^2$  of the section. Data was grouped in two major sets, one for the *Prx1*<sup>Cre/0</sup>; *Msx1*<sup>HA-His/+</sup>; *Rosa*<sup>Gli3R-Flag/+</sup>; *Gli3*<sup>Flox/+</sup> triple compound embryos and the other for the controls, and three subsets, forelimb, hindlimb and neural tube. Sets were analyzed using the Microsoft Excel 2010 software and statistical significance was evaluated using a two-tailed T test assuming unequal variance. Differences between sets were considered statistically relevant only when the p-value was inferior to 0,05.

## IV. Results

### IV.1. Overexpression of Gli3R driven by *Prx1-Cre* causes limb defects

Although previously we had verified that Cre activity driven by the *Prx1* limb enhancer element was restricted to the limb field (Fig.8), we had not tested whether this transgene would drive the expression of flagged Gli3R in the limb. Thus, in order to test the functionality of the transgene, we carried out a series of morphological analyses using heterozygous *Prx1<sup>Cre/0</sup>; Rosa<sup>Gli3R-Flag/+</sup>* and *Prx1<sup>Cre/0</sup>* control embryos and newborns. The Alcian Blue cartilage staining revealed that *Prx1<sup>Cre/0</sup>; Rosa<sup>Gli3R-Flag/+</sup>* embryos from 13.5 up to 15.5 *dpc*, displayed a series of limb abnormalities associated with growth impairment, including shortening of the three limb segments accompanied by central and/or posterior polydactily with syndactily in the autopod (Fig.10A–D and Fig.S.2). These limb malformations became even more conspicuous later during development, as shown by the Alizarin Red skeletal staining performed on 4-day old pups (P4) (Fig.10E–F).

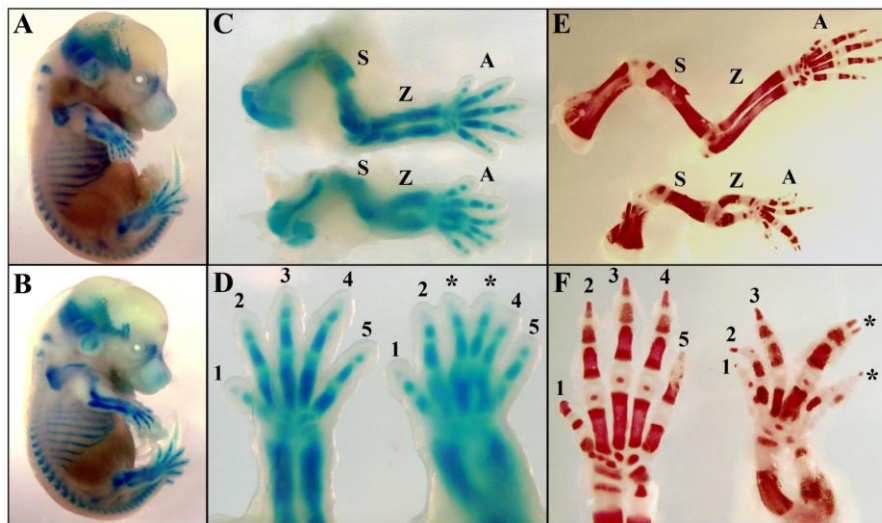


**Figure 10 Alcian Blue and Alizarin Red skeletal staining of *Prx1<sup>Cre/0</sup>; Rosa<sup>Gli3R-Flag/+</sup>* embryos and newborns.** E15.5 *Prx1<sup>Cre/0</sup>; Rosa<sup>Gli3R-Flag/+</sup>* embryos (A) display a set of limb abnormalities compared to *Prx1<sup>Cre/0</sup>* control embryos (B), including shortening of the three limb segments, specially the zeugopod (C, lower picture) and digit duplications in the autopod (D, right picture). At P4, these defects are even more striking (E, F). Forelimb controls are shown on the top (C and E) and on the left (D and F). The stylopod, zeugopod and autopod are depicted in the pictures by the letters S, Z and A, respectively. The digits – thumb to little finger – correspond to numbers 1 to 5; the digit duplications are indicated with an \*.

Noticeably, although several defects were observed at the level of the limbs, neither the embryos nor the newborns displayed any abnormalities elsewhere, indicating that the overexpression of Gli3R was active specifically in the limb field, thus proving that our construct was working properly when driven by *Prx1-Cre*. Interestingly, the abnormalities observed were much more severe in the forelimbs, comparing to the hindlimbs (Fig.S.2), which may be due to the fact that the *Prx1-Cre* transgene becomes active later in the hindlimbs, resulting in the overexpression of Gli3R to take place too late to have an early effect.

## IV.2. Gli3R and MSX1 interact *in vivo* at E11.5 in the limb bud

In order to investigate possible interactions between MSX1 and GLI3R, we started by attempting to co-immunoprecipitate both proteins from limb bud extracts prepared from E11.5 *Prx1<sup>Cre/0</sup>; Msx1<sup>HA-His/+</sup>; Rosa<sup>Gli3R-Flag/+</sup>; Gli3<sup>Flox/+</sup>* heterozygous embryos. Although we were able to detect in the IP's a band of approximately 80 kDa corresponding to GLI3R and another around 35 kDa corresponding to MSX1, we were not able to detect either of these proteins by Co-IP (data not shown), meaning that either these two proteins do not interact with each other *in vivo*, or the amount of protein complexes present is below the detection threshold of this technique. This is highly possible especially considering that all the experiments were conducted on embryos heterozygous for the tagged and flagged forms of *Msx1* and *Gli3R*, respectively. In an attempt to untangle whether this preliminary result was due to technical constraints, we decided to investigate possible *in vivo* interactions between these two proteins using Proximity Ligation Assay (PLA). For these experiments we embedded and sectioned *Prx1<sup>Cre/0</sup>; Msx1<sup>HA-His/+</sup>; Rosa<sup>Gli3R-Flag/+</sup>; Gli3<sup>Flox/+</sup>* heterozygous embryos together with *Prx1<sup>Cre/0</sup>; Msx1<sup>HA-His/+</sup>; Gli3<sup>Flox/+</sup>* control embryos. The PLA was then performed on the transverse sections containing the forelimbs, hindlimbs and the neural tube which was used as an internal negative control. The fluorescence observed and area (in mm<sup>2</sup>) on each section was quantified using the Spot Detector plugin of the Icy software. Fluorescent dots indicative of the MSX1-GLI3R interaction were detected at a high frequency in the forelimb and hindlimb mesenchyme of E11.5 embryos carrying *Msx1<sup>HA-His</sup>* and *Rosa<sup>Gli3R-Flag</sup>*, whereas almost no fluorescence was detected in the forelimbs and hindlimbs of their counterparts harboring only *Msx1<sup>HA-His</sup>* (Fig.11A'-D'). No fluorescence was detected in the dorsal region of the neural tube on both compound



mutant and control embryos, demonstrating yet again that the expression of Gli3R<sup>Flag</sup> driven by *Prx1-Cre* is restricted to the limb field (Fig.11E'–F').

The fluorescence quantification supported even further these observations by revealing that on both forelimbs and hindlimbs there were significant differences in the fluorescence density (calculated by the quotient between the number of fluorescent dots detected and the area in mm<sup>2</sup> of the sections) between compound and control embryos, whereas in the dorsal neural tube no significant differences were detected between compound and control embryos (Fig.11G). Taken together, these preliminary results support the existence of an *in vivo* interaction between MSX1 and GLI3R both in the forelimbs and hindlimbs at 11.5 *dpc*.

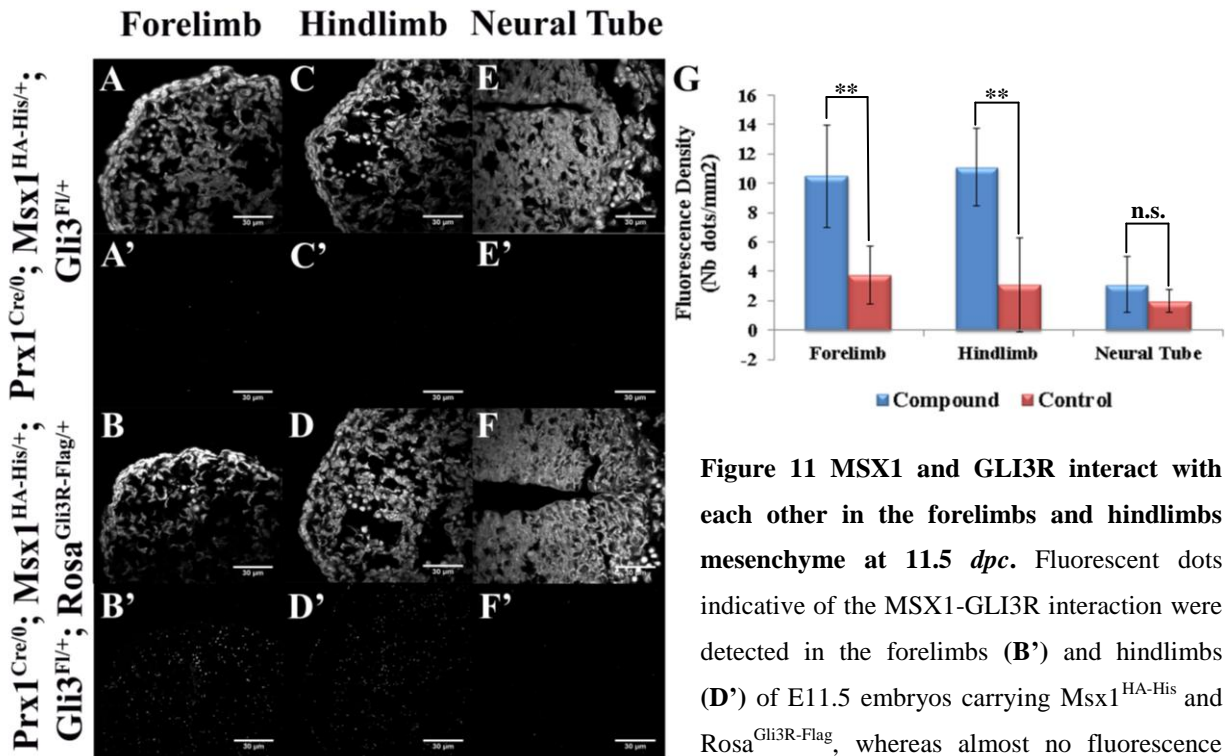


**Figure 11 MSX1 and GLI3R interact with each other in the forelimbs and hindlimbs mesenchyme at 11.5 *dpc*.** Fluorescent dots indicative of the MSX1-GLI3R interaction were detected in the forelimbs (B') and hindlimbs (D') of E11.5 embryos carrying *Msx1*<sup>HA-His</sup> and *Rosa*<sup>Gli3R-Flag</sup>, whereas almost no fluorescence

was detected in forelimbs (A') and hindlimbs (C') of their counterparts harboring only *Msx1*<sup>HA-His</sup>. No fluorescence was detected in the neural tube of both triple compound mutant (F') and control embryos (E'). The cell nuclei observed on the DAPI channel are shown in (A–F), whereas the fluorescence dots indicative of protein interactions observed on the Cy3 channel are shown in (A'– F'). The fluorescence quantification revealed that in both forelimbs and hindlimbs there were significant differences between compound and control embryos, as opposed to the neural tube (G). \*\* p-value < 0,01; n.s. non-significant. n<sub>FL</sub>=8; n<sub>HL</sub>=10; n<sub>NT</sub>=3.

### IV.3. Gli3R and Msx1 interact with the BMP pathway through Smads

These results encouraged us to pursue our protein interaction assays, this time to test the involvement of both Msx1 and Gli3R in the BMP signaling pathway via the PSmad1,5,8 protein complex. For these experiments we followed the same procedure as before, embedding and sectioning *Prx1<sup>Cre/0</sup>; Msx1<sup>HA-His/+</sup>; Rosa<sup>Gli3R-Flag/+</sup>; Gli3<sup>Flox/+</sup>* heterozygous embryos together with *Prx1<sup>Cre/0</sup>; Msx1<sup>HA-His/+</sup>; Gli3<sup>Flox/+</sup>* and *Prx1<sup>Cre/0</sup>* control embryos. The PLA was then performed on the transverse sections containing the forelimbs, hindlimbs and the neural tube which was used as an internal negative control. The fluorescence observed and area (in mm<sup>2</sup>) on each section was quantified using the Spot Detector plugin of the Icy software. Fluorescent dots indicative of the GLI3R-PSmad1,5,8 interaction were detected only in the forelimbs mesenchyme of E11.5 embryos carrying *Msx1<sup>HA-His</sup>* and *Rosa<sup>Gli3R-Flag</sup>*, whereas almost no fluorescence was detected in the forelimbs of their counterparts harboring only *Msx1<sup>HA-His</sup>* (Fig.12A'-B').

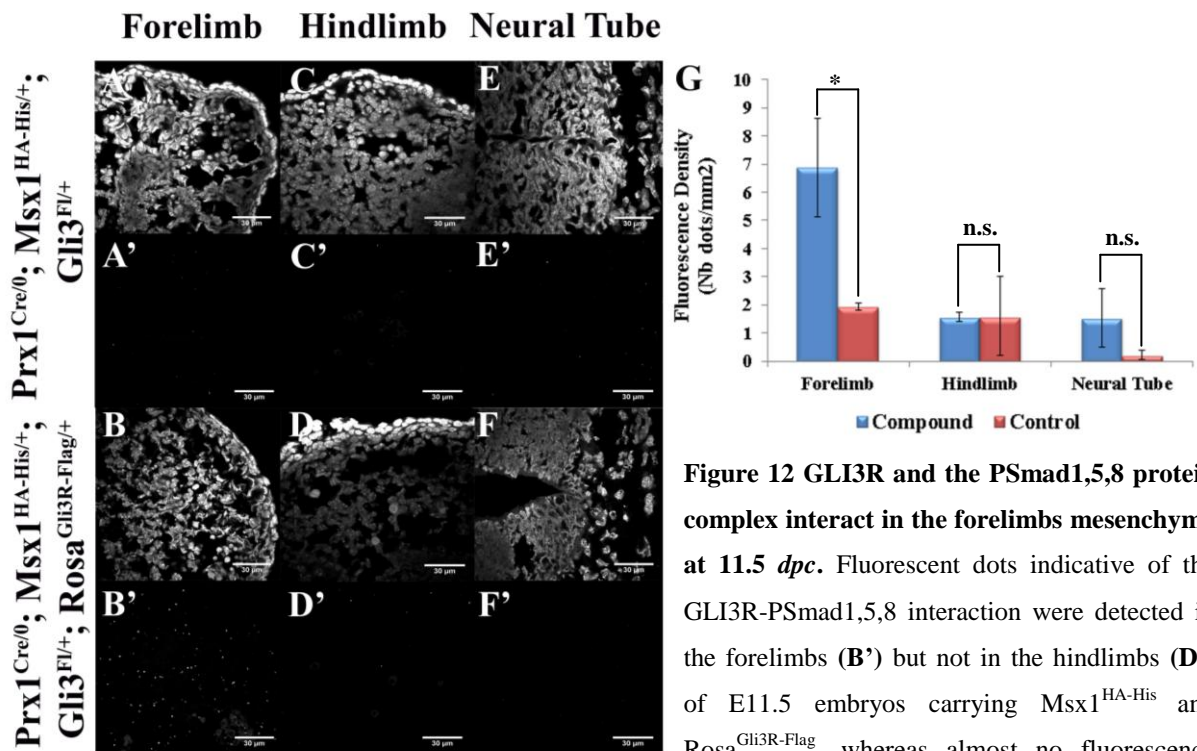


**Figure 12** GLI3R and the PSmad1,5,8 protein complex interact in the forelimbs mesenchyme at 11.5 *dpc*. Fluorescent dots indicative of the GLI3R-PSmad1,5,8 interaction were detected in the forelimbs (B') but not in the hindlimbs (D') of E11.5 embryos carrying *Msx1<sup>HA-His</sup>* and *Rosa<sup>Gli3R-Flag</sup>*, whereas almost no fluorescence

fluorescence was detected in forelimbs (A') and hindlimbs (C') of their counterparts harboring only *Msx1<sup>HA-His</sup>*. No fluorescence was detected in the neural tube of both triple compound (F') and control embryos (E'). The cell nuclei observed on the DAPI channel are shown in (A-F), whereas the fluorescence dots indicative of protein interactions observed on the Cy3 channel are shown in (A'-F'). The fluorescence quantification revealed that in the forelimbs there were significant differences between compound and control embryos, as opposed to the hindlimbs and the neural tube (G). \* p-value < 0,05; n.s. non-significant.  $n_{FL}=3$ ;  $n_{HL}=2$ ;  $n_{NT}=2$ .



No fluorescence was detected in the hindlimbs and in the dorsal region of the neural tube on both triple compound and control embryos (Fig.12C'–F'). Supporting these results, the fluorescence quantification revealed that there were statistically significant differences only in the fluorescence density between the forelimbs of compound mutant and control embryos (Fig.12G). As for MSX1-PSmad1,5,8 we observed that the fluorescent dots indicative of interaction were restricted, as in the GLI3R-PSmad1,5,8 assay, to the forelimbs of E11.5 embryos carrying both *Msx1*<sup>HA-His</sup> and *Rosa*<sup>Gli3R-Flag</sup> (Fig.13C').

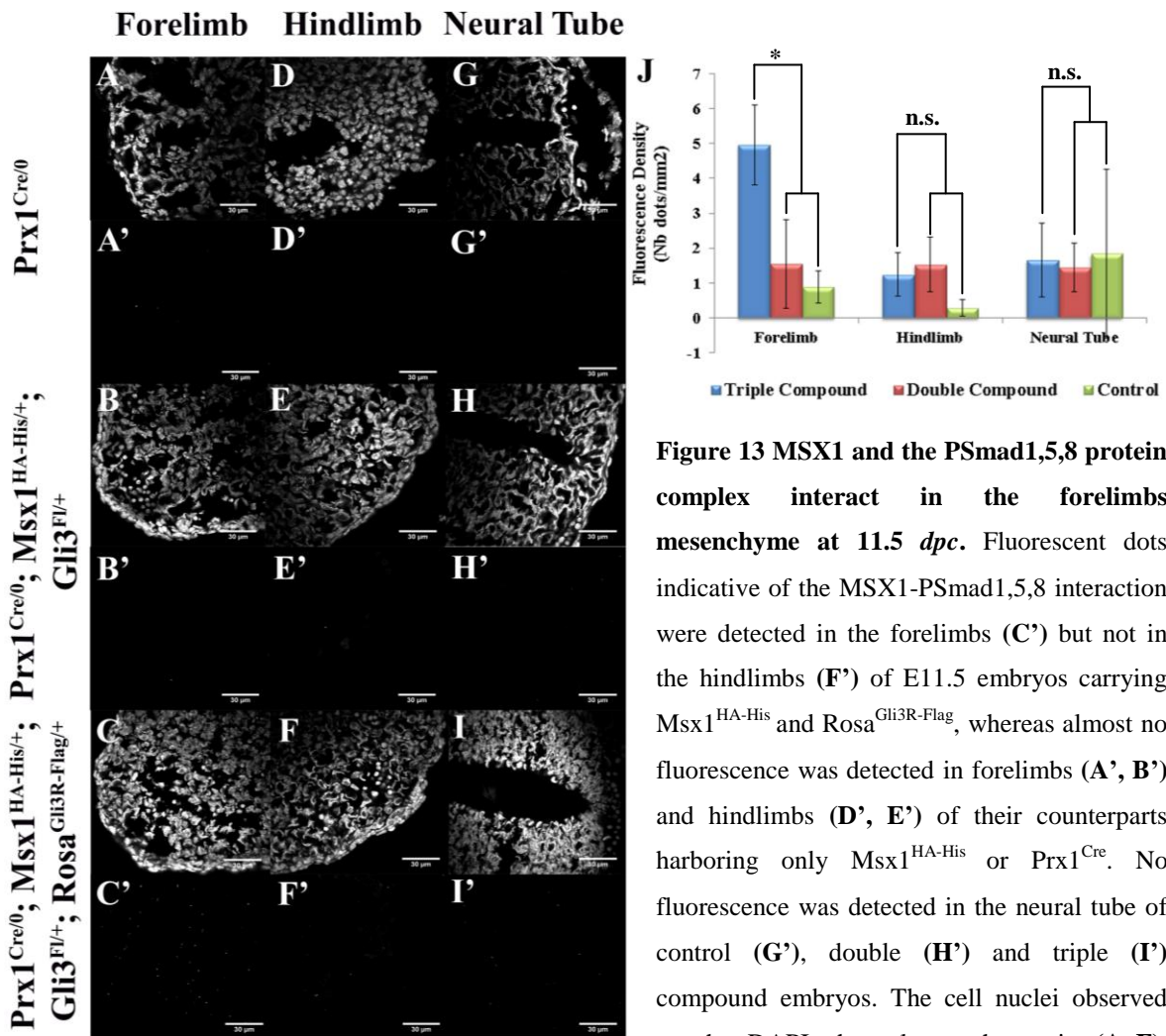


**Figure 13 MSX1 and the PSmad1,5,8 protein complex interact in the forelimbs mesenchyme at 11.5 *dpc*.** Fluorescent dots indicative of the MSX1-PSmad1,5,8 interaction were detected in the forelimbs (C') but not in the hindlimbs (F') of E11.5 embryos carrying *Msx1*<sup>HA-His</sup> and *Rosa*<sup>Gli3R-Flag</sup>, whereas almost no fluorescence was detected in forelimbs (A', B') and hindlimbs (D', E') of their counterparts harboring only *Msx1*<sup>HA-His</sup> or *Prx1*<sup>Cre</sup>. No fluorescence was detected in the neural tube of control (G'), double (H') and triple (I') compound embryos. The cell nuclei observed on the DAPI channel are shown in (A–F), whereas the fluorescence dots indicative of protein interactions observed on the Cy3 channel are shown in (A'– F').

The fluorescence quantification revealed that in the forelimbs there were significant differences between compound and control embryos, as opposed to the hindlimbs and the neural tube (J). \* p-value < 0,05; n.s. non-significant.  $n_{FL}=2$ ;  $n_{HL}=3$ ;  $n_{NT}=2$ .

Interestingly, such dots were not detected in the forelimbs of *Prx1<sup>Cre/0</sup>; Msx1<sup>HA-His/+</sup>; Gli3<sup>Flox/+</sup>* as in *Prx1<sup>Cre/0</sup>* control embryos (Fig.13A'–B'), suggesting that the interaction of Msx1 with the PSmad1,5,8 protein complex seems to be dependent on the amount of Gli3R present. As in the previous assay we could observe fluorescence neither in the hindlimbs nor in the dorsal region of the neural tube on controls, triple and double compound mutant embryos (Fig.13D'–I'), which further supports the hypothesis that Gli3R might function as an intermediate element that allows Msx1 to indirectly interact with the PSmad1,5,8 protein complex. As previously mentioned, we could only detect significant differences in the fluorescence density in the forelimbs of triple compound versus double compound and control embryos (Fig.13J).

#### IV.4. Apoptosis is deregulated in the limb bud of *Msx1<sup>-/-</sup>; Msx2<sup>-/-</sup>*

After establishing that Msx1 and Gli3R interact with each other and both are involved in the BMP signaling pathway by interacting with the PSmad1,5,8 protein complex, we were interested in investigating the processes taking place in the limb bud that could be regulated by these protein complexes. Since it had already been demonstrated that *Gli3<sup>-/-</sup>* and *Msx1<sup>-/-</sup>; Msx2<sup>-/+</sup>* mutants display limb abnormalities concomitant with apoptosis impairment (Aoto *et al.*, 2002; Lallemand *et al.*, 2009), one hypothesis that we immediately drew was that Msx1, together with Gli3R and the PSmad1,5,8 protein complex, could be involved in the control of cell death taking place in the limb bud. To investigate this possibility and confirm that Msx genes were involved in this process, females carrying *Msx1<sup>flox/flox</sup>; Msx2<sup>flox/flox</sup>* were crossed with males harboring *Msx2<sup>flox/flox</sup>* together with the *Msx1<sup>CreERT2</sup>* transgene, that allows the activation of Cre recombinase upon injection of Tamoxifen exclusively at sites where Msx1 is expressed. Using this strategy, we were able to generate *Msx1<sup>-/-</sup>; Msx2<sup>-/-</sup>* viable embryos as these genes were only defloxed at 8.5 *dpc* (the time point selected for Tamoxifen injection). To analyse the distribution and extent of apoptosis in the limb bud at 12.5 *dpc*, we performed immunofluorescence on transverse sections against Caspase3 in *Msx1<sup>-/-</sup>; Msx2<sup>-/-</sup>* and *Msx1<sup>CreERT2/+</sup>; Msx2<sup>-/+</sup>* control embryos. This experiment revealed that whereas in the controls apoptosis is present on both the anterior and posterior extremities of the hindlimb bud (Fig.14A' and C'), in the double *Msx1<sup>-/-</sup>; Msx2<sup>-/-</sup>* mutant cell death is practically absent on the anterior region and maintains its distribution on the posterior (Fig.14B' and D'), which may account for the anterior overgrowth observed in the

hindlimbs of double *Msx1*<sup>-/-</sup>; *Msx2*<sup>-/-</sup> mutant embryos (data not shown). Taken together, these results clearly confirm that *Msx* genes are required for the control of apoptosis taking place during the earliest developmental phases of limb formation, and ultimately for the morphogenetic events responsible for modulating its final shape. Whether this involvement of *Msx* is accompanied by the intervention of Gli3R and elements of the BMP signaling cascade also pointed out to be involved in cell death control, requires further investigation.

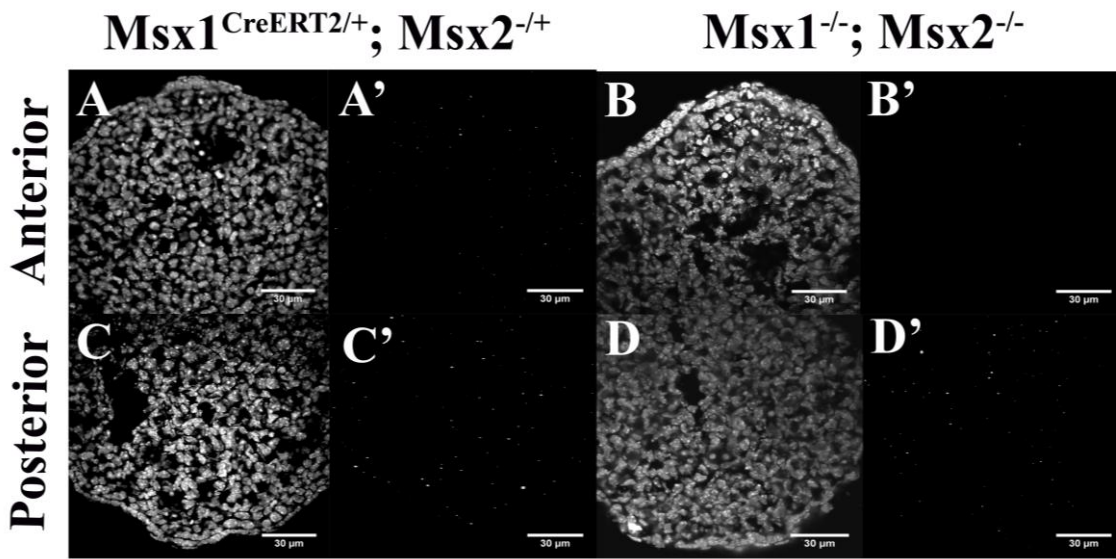


**Figure 14 Apoptosis is impaired in the limb bud of *Msx1*<sup>-/-</sup>; *Msx2*<sup>-/-</sup> double mutants.** The immunofluorescence against Caspase3 revealed that whereas in the *Msx1*<sup>CreERT2/+</sup>; *Msx2*<sup>-/+</sup> control embryos apoptosis is present on both the anterior and posterior extremities of the hindlimb bud (A', C'), in the double *Msx1*<sup>-/-</sup>; *Msx2*<sup>-/-</sup> mutant cell death is practically absent on the anterior region (B') and maintains its distribution on the posterior end of the limb bud (D'). The cell nuclei observed on the DAPI channel are shown in (A–D), whereas the expression pattern of Caspase3 observed on the Alexa Fluor 488 channel are shown in (A'–D').

**Courtesy of Mathura Shanmugasundaram, PhD.**

## V. Discussion

### V.1. The relationship between Msx1, Gli3R and the BMP cascade

In the present work we provide evidence that supports the hypothesis stating that Msx1 and Gli3R interact *in vivo* in the forelimb and hindlimb buds at 11.5 *dpc*. Afterwards, we were able to show that these transcription factors interact with the PSmad1,5,8 protein complex, the intracellular transducer of the BMP signaling pathway. And finally we demonstrated that *Msx* genes are required for the control of apoptosis taking place during the earliest developmental phases of limb formation. Based on these results and on the fact that the BMP signaling pathway has been systematically implicated in the apoptotic events taking place in the murine and in the avian limb as well (Guha *et al.*, 2002; Yokouchi *et al.*, 1996; Zou and Niswander, 1996), together with the observation that the absence of *Msx* genes and/or *Gli3* induce the loss of the anterior apoptotic domain normally observed during the earliest phases of limb development (Aoto *et al.*, 2002; Lallemand *et al.*, 2009), we propose that Msx1, Gli3R and the PSmad1,5,8 protein complex interact with each other in order to form a trimeric nuclear transcriptional complex that will drive the expression of BMP target genes directly involved in cell death regulation.

Noticeably, although some Gli3R still formed from the endogenous *Gli3* locus, in the absence of *Rosa<sup>Gli3R-Flag</sup>* we were not able to detect an interaction between Msx1 and the PSmad1,5,8 protein complex, suggesting that the Msx1-PSmad1,5,8 interaction is dependent on the amount of Gli3R present. This assumption is perfectly logical, considering the fact that these embryos possess only one *Gli3* endogenous allele capable of generating Gli3R, which is the only source of this transcriptional repressor, since no artificial Gli3R is present. As a result, the amount of Gli3R present is greatly reduced compared to the situation where *Rosa<sup>Gli3R-Flag</sup>* is also present and much fewer Msx1-PSmad1,5,8 interactions form. Thus, one possible explanation is that the reduction in the number of interactions is so accentuated that the few interactions taking place under these conditions become undetectable, as they may be below the detection threshold of the PLA.

It is also likely that this detection threshold issue is being amplified by the relative strengths of the *Gli3* and the *Rosa26* promoters that are driving the expression of the

endogenous and the artificial Gli3R, respectively. Although the *Rosa26* locus is traditionally used for constitutive and ubiquitous gene expression due to its strong promoter element, in this case it is not known whether this promoter is more or less strong compared to the endogenous Gli3 promoter. However, if indeed the *Rosa26* promoter is stronger than the Gli3 endogenous promoter, then the artificial Gli3R will be more expressed compared to its endogenous counterpart. As a consequence, it is easy to imagine that when *Rosa<sup>Gli3R-Flag</sup>* is not present, the Gli3R expression level driven solely by the endogenous less strong Gli3 promoter will significantly decrease.

Furthermore, we also need to consider the possibility that the artificial Gli3R protein driven by the *Rosa26* promoter may have a higher turnover rate compared to the endogenous protein, since the endogenous Gli3R is produced only after processing of the full-length Gli3, a process that the artificial Gli3R does not undergo, thus saving a substantial amount of time required for protein synthesis. Therefore, in the absence of *Rosa<sup>Gli3R-Flag</sup>*, the Gli3R turnover rate will suffer a drastic reduction that combined with a possible less strong endogenous promoter, and only one Gli3 allele present, will result in the decrease of Gli3R present in the limb bud. Subsequently, this will lead to the formation of fewer Msx1-PSmad1,5,8 interactions that may not be detected, as they are below the detection threshold of this technique.

Although this explanation is still unclear and requires further investigation in the future, these observations are clearly suggesting that either Gli3R acts as an intermediary element that mediates the indirect interaction between Msx1 and the PSmad1,5,8 protein complex by interacting simultaneously with both proteins (Fig.15A), or Gli3R is one of the members of a trimeric transcriptional complex where the three proteins bind and interact with each other, that cannot be assembled nor perform its transcriptional functions in the absence of one single element (Fig15B).

Although in the two previous models Gli3R is undoubtedly an essential element whose presence is necessary for these protein interactions to take place, the role of Msx1 is less clear. Whereas in the first model Msx1 seems to be only required as an accessory cofactor for BMP-mediated apoptosis to occur (Fig.15A), in the second model Msx1 interacts with Gli3R and the PSmad1,5,8 protein complex simultaneously and is required for the activity of the trimeric transcriptional protein complex (Fig.15B). In order to clarify the role of Msx1 in the trimeric transcriptional nuclear complex a protein interaction assay testing the ability of Gli3R to interact with the PSmad1,5,8 protein

complex could be performed on embryos lacking both the endogenous Msx1 and the artificial *Msx1*<sup>HA-His</sup> allele. Although time and technical constraints prevented us from performing this experiment, we can argue that if in fact this interaction took place in the absence of any form of Msx1, then we could safely state that Msx1 acts merely as a cofactor in this trimeric transcriptional complex and it is not required for its activity. If, on the other hand, this interaction did not occur, then we could say that Msx1 is necessary for the trimeric transcriptional complex to form, and subsequently for its transcriptional activity.

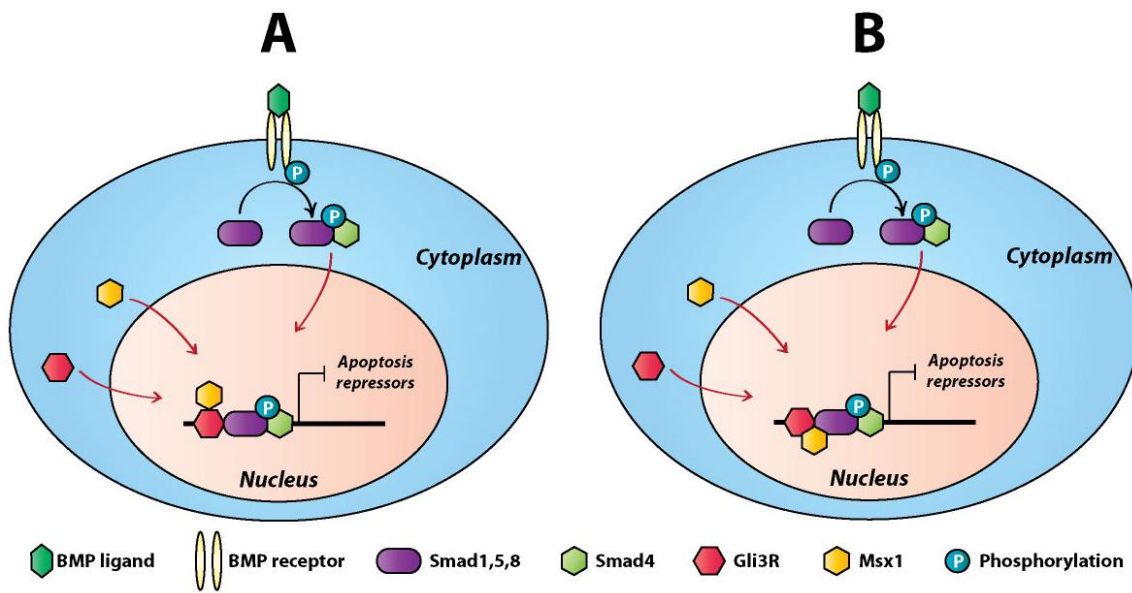


**Figure 15 Proposed models to explain how Msx1 and Gli3R interact with the PSmad1,5,8 protein complex in order to drive BMP-mediated apoptosis in the forelimb bud.** On both models upon ligand binding the Smad1,5,8 protein complex is phosphorylated by the intracellular domain of the BMP receptor. Afterwards, the PSmad1,5,8 protein complex associates with Smad4 and is translocated into the cell nucleus. In the meantime, the Msx1 and Gli3R transcription factors synthesized in the cytoplasm migrate and enter the cell nucleus. In the nucleus the PSmad1,5,8 (together with Smad4), Gli3R and Msx1 associate, forming a trimeric transcriptional complex that will actively repress the expression of apoptosis repressors, which will trigger cell death in cells where BMP signaling is active. Whereas in (A) Msx1 interacts only with Gli3R and acts as a cofactor, in (B) Msx1 is one of the elements composing the trimeric transcriptional complex where all the three proteins interact with each other and its presence is required for its transcriptional activity. The red arrows depict the cytoplasm-to-nucleus translocations.

Alternatively, to uncover which scenario would be more likely to correspond to the *in vivo* situation, one could also investigate the protein domains and motifs that allow the physical interactions between these proteins. Whereas it has been pointed out that the



zinc-finger region of the Gli3 protein seems to act as a binding domain for Smad proteins (Liu *et al.*, 1998), regions involved in mediating Msx1-Gli3R and Msx1-PSmad1,5,8 interactions remain to be discovered.

Another interesting aspect we did not investigate and ought to be explored has to do with the role each protein plays in the trimeric transcriptional complex and its consequences in terms of gene expression. It is known that the PSmad1,5,8 protein complex can induce and also repress transcription of BMP target genes, depending on the transcription factors and cofactors it binds to, whereas Gli3R and Msx1 are potent transcription repressors (Catron *et al.*, 1995; Zwijsen *et al.*, 2003). It is thus plausible to admit that upon binding to transcription factors that actively repress transcription, the PSmad1,5,8 protein complex will promote the repression of BMP target genes. One possibility that correlates with our previous observations is that upon assembling, this trimeric nuclear transcriptional complex would actively repress the expression of apoptosis repressors, which would trigger cell death in cells where BMP signaling is active.

Also, the fact that *Gli3*<sup>-/-</sup> and *Msx1*<sup>-/-</sup>; *Msx2*<sup>+/-</sup> mutants display limb abnormalities concomitant with apoptosis impairment (Aoto *et al.*, 2002; Lallemand *et al.*, 2009) seems to support the idea that in the absence of a single element, the trimeric transcriptional complex does not assemble and it is not able to relieve the repression over genes involved in apoptosis. Although this scenario may seem more likely considering these new set of observations, the model admitting that Msx1 may act only as an accessory cofactor for BMP-mediated apoptosis to occur cannot be discarded at this point.

Another aspect that should be properly analyzed is the temporal and spatial profile of the BMP-mediated apoptosis. Our results clearly demonstrate that these three proteins interact with each other in mesenchymal cells of the forelimbs at 11.5 *dpc*, which corresponds to the stage where cells start undergoing apoptosis in the limb field. Although we were able to detect an interaction between Gli3R and Msx1 in the hindlimbs of *Prx1*<sup>Cre/0</sup>; *Msx1*<sup>HA-His/+</sup>; *Rosa*<sup>Gli3R-Flag/+</sup>; *Gli3*<sup>Flox/+</sup> compound embryos, we were not able to detect any interaction between these transcription factors and the PSmad1,5,8 in the hindlimbs of the same embryos. This may be explained admitting that BMP-mediated apoptosis is initiated at a later stage in the hindlimbs that have a developmental delay of half a day compared to the forelimbs. The fact that these two

transcription factors start interacting with each other before interactions with the PSmad1,5,8 can be detected, may indicate that both of them are involved in other developmental events occurring in the limb field before BMP-mediated apoptosis takes place.

## V.2. Concluding remarks

In the future, the molecular and cellular nature of these protein interactions taking place in the limb field should be investigated in more detail, aiming to:

1. Obtain more clear-cut results regarding the role of Gli3R in the trimeric nuclear transcriptional complex, by generating a *Prx1*<sup>Cre/Cre</sup>; *Msx1*<sup>HA-His/HA-His</sup>; *Rosa*<sup>Gli3R-Flag/Gli3R-Flag</sup>, *Gli3*<sup>Flox/Flox</sup> homozygous transgenic line that would enable to perform all the interaction assays in the absence of endogenous Gli3
2. Elucidate the role of Msx1 in BMP-mediated apoptosis
3. Discover the protein domains and motifs that allow the physical interactions between these proteins to take place
4. Untangle how these protein interactions modulate gene expression and what are the consequences in terms of limb morphogenesis
5. Investigate in more detail the temporal and spatial profile of BMP-mediated apoptosis in the limb
6. Discover other transcription factors and/or cofactors involved in BMP-mediated apoptosis regulation



# References

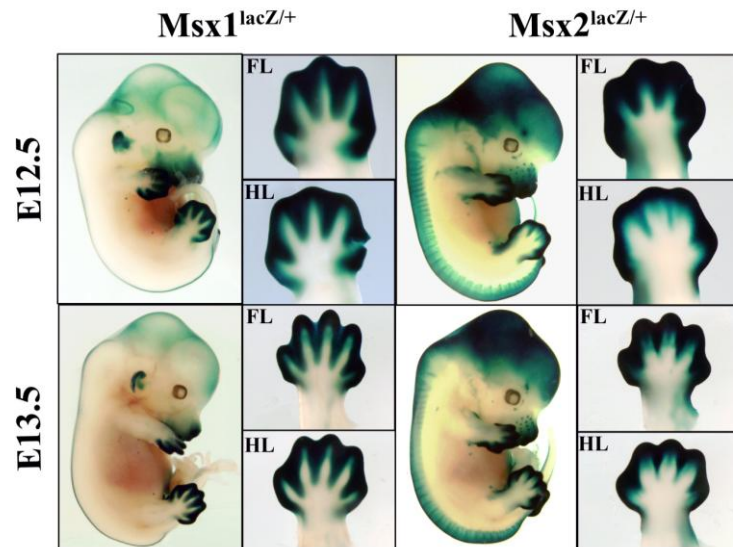
- Ahn, S. and Joyner, A. L.** (2004). Dynamic changes in the response of cells to positive hedgehog signaling during mouse limb patterning. Cell **118**, 505-16.
- Aoto, K., Nishimura, T. et al.** 2002. Mouse GLI3 Regulates Fgf8 Expression and Apoptosis in the Developing Neural Tube, Face, and Limb Bud. Developmental Biology **251**(2): 320-332.
- Bénazet, J. and Zeller, R.** 2009. Vertebrate Limb Development: Moving from classical morphogen gradients to an integrated 4-dimensional patterning system. Cold Spring Harb Perspect in Biology.
- Bensoussan-Trigano, V., Lallemand, Y. et al.** 2011. Msx1 and Msx2 in limb mesenchyme modulate digit number and identity. Developmental Dynamics **240**(5): 1190-1202.
- Berge, D., Brugmann S., Helms J., and Nusse R.** 2008. Wnt and FGF signals interact to coordinate growth with cell fate specification during limb development. Development **135**(19): 3247-3257.
- Blaess S, Stephen D, Joyner AL.** 2008. Gli3 coordinates three-dimensional patterning and growth of the tectum and cerebellum by integrating Shh and Fgf8 signaling. Development **135**:2093–2103.
- Bowers, M., Eng, L. et al.** 2012. Limb anterior–posterior polarity integrates activator and repressor functions of GLI2 as well as GLI3. Developmental Biology **370**(1): 110-124.
- Catron, K., Zhang, H. et al.** 1995. Transcriptional Repression by Msx-1 Does Not Require Homeodomain DNA-Binding Sites. Molecular and Cellular Biology **15**(2): 861-871.
- Chiang, C., Litlington, Y. et al.** 2001. Manifestation of the Limb Prepattern: Limb Development in the Absence of Sonic Hedgehog Function. Developmental Biology **236**(2): 421-435.

- Davidson, D.R., Crawley, A., Hill, R.E., Tickle, C.,** 1991. Position-dependent expression of two related homeobox genes in developing vertebrates limbs. Nature **352**: 429–431.
- Guha, U., Gomes, W. *et al*** 2002. *In Vivo* Evidence That BMP Signaling Is Necessary for Apoptosis in the Mouse Limb. Developmental Biology **249**, 108–120
- Hall, B. K. and Miyake, T.** 2000. All for one and one for all: condensations and the initiation of skeletal development. BioEssays **22**, 138-147.
- Harfe, B., Scherz, P., Nissim, S. *et al.*** 2004. Evidence for an expansion-based temporal Shh gradient in specifying vertebrate digit identities. Cell **118**: 517-528.
- Kang, S., Graham, J., Olney, A. and Biesecker, L.** 1997. GLI3 frameshift mutations cause autosomal dominant Pallister-Hall syndrome. Nature Genetics 266–268
- Kimelman, D.** 2006. Mesoderm induction: from caps to chips. Nat Rev Genet **7**(5): 360-372.
- Kraus, P., Fraidenraich, D. *et al.*** 2001. Some distal limb structures develop in mice lacking Sonic hedgehog signaling. Mechanisms of Development **100**(1): 45-58.
- Lallemand, Y., Nicola, M. *et al.*** 2005. Analysis of Msx1; Msx2 double mutants reveals multiple roles for Msx genes in limb development. Development **132**(13): 3003-3014.
- Lallemand, Y., Bensoussan, V. *et al.*** 2009. Msx genes are important apoptosis effectors downstream of the Shh/Gli3 pathway in the limb. Developmental Biology **331**(2): 189-198.
- Lee, J., Platt, K. A., Censullo, P. and Ruiz A.** 1997. Gli1 is a target of Sonic hedgehog that induces ventral neural tube development. Development (Cambridge, England).
- Lewis, P., Dunn, M., McMahon, J. *et al.*** 2001. Cholesterol modification of sonic hedgehog is required for long-range signaling activity and effective modulation of signaling by Ptc1. Cell **105**: 599-612.
- Litingtung, Y., Dahn, R., Li, Y. *et al.*** 2002. Shh and Gli3 are dispensable for limb skeleton formation but regulate digit number and identity. Nature **418**: 979–983

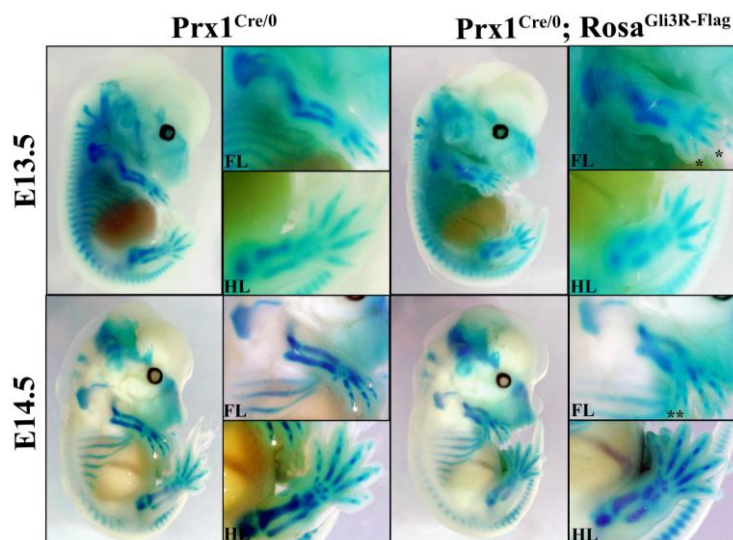
- Liu, F., Massagué, J., Altaba, A.** 1998. Carboxy-terminally truncated Gli3 proteins associate with Smads. Nature Genetics p. 325–6
- Liu, W., Sun, X., Braut, E. *et al.*** 2005. Distinct functions for Bmp signaling in lip and palate fusion in mice. Development **132**: 1453-1461
- Logan, M., Martin, J. F. *et al.*** 2002. Expression of Cre recombinase in the developing mouse limb bud driven by a Prxl enhancer. genesis **33**(2): 77-80.
- Ovchinnikov, D., Selever, J., *et al.*** 2006. BMP receptor type IA in limb bud mesenchyme regulates distal outgrowth and patterning. Developmental Biology **295**(1): 103-115.
- Riddle, R., Johnsom, R., Laufer, E. *et al.*** 1993. Sonic hedgehog mediates the polarizing activity of the ZPA. Cell **75**: 1401-1416.
- Robert, B., Lyons, G., Simandl, B.K., Kuroiwa, A., Buckingham, M.,** 1991. The apical ectodermal ridge regulates Hox-7 and Hox-8 gene expression in developing chick limb buds. Genes Dev. **5**: 2363–2374.
- Robert, B. and Lallemand, Y.** 2006 Anteroposterior Patterning in the Limb and Digit Specification: Contribution of Mouse Genetics. Developmental Dynamics **235**:2337–2352
- Ros, M. and Fernandez-Teran, M.** 2008. The apical ectodermal ridge: morphological aspects and signaling pathways. Int. J. Dev. Biol.; **52**: 857-871.
- Taher L., Collette, N.M., Muruges, D., Maxwell, E., Ovcharenko, I., *et al.*** 2011. Global Gene Expression Analysis of Murine Limb Development. PLoS ONE **6**(12): e28358.
- te Welscher, P., Zuniga, A., Kijper, *et al.*** 2002. Progression of vertebrate limb development through SHH-mediated counteraction of GLI3. Science **298**, 827-830
- Towers, M. and Tickle, C.** 2009. Growing models of vertebrate limb development. Development **136**(2): 179-190.
- Vokes, S. A., Ji, H. *et al.*** 2008. A genome-scale analysis of the cis-regulatory circuitry underlying sonic hedgehog-mediated patterning of the mammalian limb. Genes & Development **22**(19): 2651-2663.

- Wang, B., Fallon, J. F. and Beachy, P. A.** (2000). Hedgehog-regulated processing of Gli3 produces an anterior/posterior repressor gradient in the developing vertebrate limb. Cell **100**, 423-34.
- Wolpert, L.** (1969). Positional information and the spatial pattern of cellular differentiation. J Theor Biol **25**, 1-47.
- Yokouchi, Y., Sakiyama, et al.** 1996. BMP-2/-4 mediate programmed cell death in chicken limb buds. Development **122**, 3725–3734.
- Zeller, R.** 2004. It Takes Time to Make a Pinky: Unexpected Insights into How SHH Patterns Vertebrate Digits. Sci. STKE **259**: pe53
- Zeller, R. and Zuniga, A.** 2007. Shh and Gremlin1 chromosomal landscapes in development and disease. Current Opinion in Genetics & Development **17**(5): 428-434.
- Zeller R., Lopez-Rios J., Zuniga A.** 2009. Vertebrate limb bud development: moving towards integrative analysis of organogenesis. Nature Rev Genet **10**: 845–858.
- Zhang, Z., Song, Y. et al.** 2002. Rescue of cleft palate in Msx1-deficient mice by transgenic Bmp4 reveals a network of BMP and Shh signaling in the regulation of mammalian palatogenesis. Development **129**(17): 4135-4146.
- Zou, H., and Niswander, L.** 1996. Requirement for BMP signaling in interdigital apoptosis and scale formation. Science **272**, 738–741.
- Zwijsen, A., Verschuere, K. et al.** 2003. New intracellular components of bone morphogenetic protein/Smad signaling cascades. FEBS Letters **546**, 133–139.

## Appendix I – Supplementary data



**S1. Expression of *Msx1* and *Msx2* visualized in whole-mount at E12.5 and E13.5, using the *lacZ* reporter.** *Msx1* (left panel) and *Msx2* (right panel) continue to be highly expressed in the distal region of the limb bud, in the central nervous system and in the olfactory bulb at later developmental stages, as they were at E11.5. The forelimb (FL) and hindlimb (HL) of each embryo are shown beside each panel.



**S2. Alcian Blue staining of *Prx1*<sup>Cre/0</sup>; *Rosa*<sup>Gli3R-Flag/+</sup> embryos.** E13.5 and E14.5 *Prx1*<sup>Cre/0</sup>; *Rosa*<sup>Gli3R-Flag/+</sup> embryos (right panel) display a set of limb abnormalities comparing to *Prx1*<sup>Cre/0</sup> control embryos (left panel), including shortening of the three limb segment and digit duplications in the autopod (D, right picture). The forelimb (FL) and hindlimb (HL) of each embryo are shown beside each panel. The digit duplications are indicated with an \*.

## Appendix II – Solutions and buffers

Table 6 Common solutions and buffers.

Common Solutions	
Solution	Composition
<b>PBS 1X</b>	8g 137 mM NaCl
	0,2g 2.7 mM KCl
	1,44g 10 mM Na <sub>2</sub> HPO <sub>4</sub>
	0,24g 1.8 mM KH <sub>2</sub> PO <sub>4</sub>
	Distilled water qsp 1L
	Adjust pH to 7.4
<b>PBS-1% BSA 5%-GS-0,5% Triton X100</b>	5 mL 10% BSA
	2,5 mL GS
	1,25 mL Triton X100 20%
	PBS qsp 50 mL
<b>PBS-0,2% Triton X100</b>	1,0 mL Triton X100 20%
	PBS qsp 50 mL
<b>PBS-0.1% Tween-20</b>	50 µL 100% Tween-20
	PBS qsp 50 mL
<b>70% Ethanol</b>	35 mL 100% Ethanol
	Distilled water qsp 50 mL
<b>80% Ethanol-20% Acetic Acid</b>	40 mL 100% Ethanol
	10 mL 1M Acetic acid
<b>70% Ethanol-1% HCl</b>	35 mL 100% Ethanol
	1,33 mL 37,5% HCl
	Distilled water qsp 50 mL
<b>1% NaOH</b>	40g 1M NaOH
	Distilled water qsp 1L
<b>0,01% NaOH</b>	100 mL 1% NaOH
	Distilled water qsp 1L
PCR Solutions	
Solution	Composition
<b>Loading buffer</b>	15g Sucrose
	0,5 mL 50 mM Red Cresol
	Distilled water qsp 25 mL
<b>Extraction buffer</b>	125 µL 10M NaOH
	20 µL 0.5M EDTA
	Distilled water qsp 50 mL
<b>Neutralization buffer</b>	2 mL 1M Tris-HCl
	Distilled water qsp 50 mL

**Table 7 Solutions and buffers used in protein extraction, Co-IP and WB.**

<b>Protein Extraction and Co-IP</b>	
<b>Solution</b>	<b>Composition</b>
<b>Lysis Buffer</b>	200 µL 1M Hepes, pH 7.8
	3 µL 0.5M EDTA
	100 µL 1M KCl
	4 mL 1M NaCl
	1 mL NP40 10%
	100 µL 100 mM DTT
	Distilled water qsp 10 mL
	Add 1 tablet protease inhibitors
<b>0.1M Sodium-Acetate, pH5.0</b>	28,82 mL 1M Acetic acid
	273,3 mL 0.3M Sodium acetate
	Distilled water qsp 1L
	Adjust pH to 5.0
<b>50 mM Tris-buffered saline, pH7.5</b>	6,35 g Tris-HCl
	1,18 g Tris-base
	8,77 g NaCl
	Distilled water qsp 1L
	Adjust pH to 7.5
<b>0.1M Citrate, pH2.0</b>	21,01g 1M citric acid
	Distilled water qsp 1L
	Adjust pH to 2.0
<b>Laemlli-5%β-mercaptoethanol</b>	50 µL β-mercaptoethanol
	950 µL 1X Laemlli sample buffer
<b>Western Blot</b>	
<b>Solution</b>	<b>Composition</b>
<b>TBS 10X, pH7.6</b>	22,20g Tris-base
	80g NaCl
	Distilled water qsp 1L
	Adjust pH to 7.6
<b>TBS-0.1% Tween-20</b>	500 µL 100% Tween-20
	TBS 1X qsp 500 mL
<b>TBS-0.1% Tween-20-5% Milk</b>	50 µL 100% Tween-20
	2,5g Régilait milk
	TBS 1X qsp 50 mL
<b>Tris-Glycine-SDS Running Buffer 10X</b>	30g Tris-base
	144g Glycine
	100 mL 10% SDS
	Distilled water qsp 1L
<b>Transfer Buffer (semi-dry transfer) 1X</b>	5,82g Tris-base
	2,93g Glycine
	3,75 mL 10% SDS
	200 mL 100% Ethanol
	Distilled water qsp 1L



**Table 8 Solutions and buffers used in Alcian Blue, Alizarin Red and X-Gal staining.**

<b>Staining Solutions</b>	
<b>Solution</b>	<b>Composition</b>
<b>Alizarin Red</b>	50 mg Alizarin red (Sigma Aldrich)
	0,1% NaOH qsp 1L
<b>Alcian Blue</b>	5 mL Alcian Blue 8GX
	7 mL 1M Acetic acid
	10 mL Distilled water
	38 mL 100% Ethanol
<b>X-Gal</b>	1 mL 50 mM $K_4Fe(CN)_6$ /50 mM $K_3Fe(CN)_6$
	20 $\mu$ L 1M $MgCl_2$
	100 $\mu$ L 1% NP40
	100 $\mu$ L 1% Deoxycholate
	1 mL PBS 10X
	250 $\mu$ L 4% X-Gal
	7,53 mL Distilled water

## Appendix III – Antibodies

**Table 9 Primary and secondary Antibodies used in PLA and immunofluorescence.**

<b>Antibody</b>	<b>Dilution</b>	<b>Reference</b>
Rabbit polyclonal Primary Anti-HA	1:500	Sigma Aldrich, ref: H6908
Rabbit polyclonal Primary Anti-Caspase3	1:100	Cell Signaling Technology , ref: #9662
Rabbit polyclonal Primary Anti-PSmad1,5,8	1:500	Santa Cruz Biotechnology, ref: sc-63031-R
Mouse monoclonal Primary Anti-HA	1:50	Covance Research Products Inc, ref: MMS-101P
Mouse monoclonal Primary Anti-Flag	1:50	Sigma Aldrich, ref: F1804
Secondary Alexa Fluor 488 <sup>®</sup> goat anti- mouse IgG	1:300	Invitrogen, ref: A-11001